CHALMERS
UNIVERSITY OF TECHNOLOGY

Master thesis

Techno-economic analysis of integrated heat recovery applications for a thermal energy storage system based on an aluminum alloy

for the degree of Master of Science (M. Sc.) in the Master's program: Sustainable Energy Systems

by Marcus Peter

Chalmers University of Technology
Göteborg, Sweden 2022
Department of Space, Earth and Environment
Division of Energy Technology

Corporate Supervisor:	Hans Svanbom
Examiner:	Prof. Simon Harvey
Academic Supervisor:	M.Sc. Christian Lagner

Table of contents

1. Abstract

Throughout this thesis, a techno-economical model was constructed to assess the economic benefit of incorporating an energy storage technology capable of functioning in CHP mode in conjunction with solar power into the energy systems of various applications. The thesis was completed in collaboration with Azelio AB, a Gothenburg-based energy storage company, with the aim of determining the economic worth of the heat generated by their CHP capable energy storage technology, alias the TES.POD. Before more computationally expensive modeling is conducted, the model serves as a preliminary tool for the company to identify potential applications where the TES.POD in a CHP operation may be economically feasible.

The methodology was successfully applied in three case studies across different industry sectors.

2. Introduction

Throughout human history, primary energy resources have been converted to more useful energy carriers, such as heat and electricity. Before the industrial revolution, energy consumption only included biomass, see figure 1. With the discovery of higher energy content resources, such as fossil fuels, a new age in human history dawned. The living conditions of mankind improved and the total population on earth grew rapidly. The global consumption of useful energy grew rapidly as did the consumption of fossil fuels. In the last hundred years, it has become clear that combustion of fossil fuels is causing global changes in the climate. Since then, humanity has been faced with the challenge of replacing fossil fuels with climate-friendly energy resources without sacrificing quality of life. In 2015, the majority of countries signed the Paris Agreement to keep global temperature rise below 2 °C, compared to pre-industrial levels.

Substantial improvements towards reaching the goal to mitigate climate change have been made. Mainly the rapid development of non-fossil fuel based power technologies, such as wind- and solar power, contributed to this. They went through a rapid development and gained shares in the energy supply market in a short time. Their ability to produce low cost electricity resulting from their low operational cost is forcing fossil fuel power plants out of the market. But their superiority with respect to cost is overshadowed by their reliance on external factors, such as wind and sunlight. The intermittent nature of wind- and solar power is introducing new challenges to operators of power grid systems, which sooner or later will limit the further instalment of capacity in the power grid system.

However, zero-emissions from the power system are indispensable in order to reach the climate goals, which means the problems associated with renewable energy sources need to be dealt with. Energy storage technologies represent a part of the solution. They have the capability to reduce the unreliability aspect, coming from introducing high shares of renewable power sources, by complementing renewables at times when power output from these technologies is not possible.

This thesis was conducted in collaboration with Azelio AB. The company has recently developed an innovative thermal heat storage technology, which charges and discharges electricity coming from renewable sources. Azelio's Thermal Energy Storage, Power on Demand, alias TES.POD, provides, besides electricity, low temperature heat during discharge. The company sees potential value for this excess heat and is thus seeking opportunities to enter the Combined Heat & Power market. The purpose of this thesis was to analyze its economic value by developing a techno-economical model that is able to identify and evaluate potential applications where the TES.POD could be economically valuable.

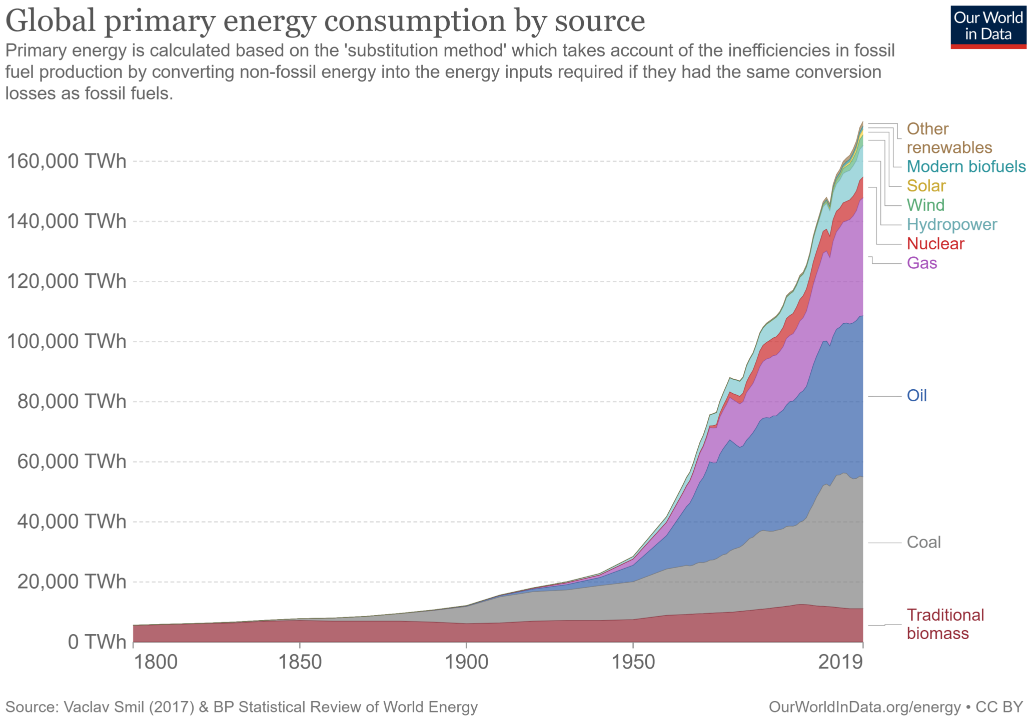

Figure 1: Global primary energy consumption by source [Smil, 2016]

2.1. Azelio

Azelio AB is a Swedish company focused on harnessing renewable energy sources using Stirling engine technology. The company has its headquarters in Gothenburg, its manufacturing site in Uddevalla and its R&D site in Åmål, Sweden.

In 2018, the company introduced an innovative thermal energy storage technology to complement their Stirling engine technology. The product is unique in the energy storage sector, using comparatively environmentally friendly and abundant materials, such as recycled aluminum as a phase-changing storage medium. The company offers a cost-competitive size to energy efficient storage option in a market mostly dominated by electricity batteries and pumped hydropower. The company is focusing on Long Duration Energy Storage as defined in the LDES Council [LDES Council, 2022].

One TES.POD unit has a rated power output of 13 kW and is capable to continuously discharge power for up to 13 h. The technology is scalable by for instance connecting multiple units in series and thus can provide energy up to MW dimensions.

The company offers potential customers a complete renewable energy system by jointly redesigning the energy system of the customer with renewables, such as solar power, and the TES.POD as an electricity storage medium.

2.2. Objective of project

The objective of this thesis is to develop a tool for conducting a techno-economic analysis of Azelio's TES.POD in CHP configuration for case by case applications. In addition to electricity, the TES.POD produces low-temperature heat, which is currently in the process of commercialization. The aim of the thesis is to investigate the potential economic value of using the excess heat in various market sectors.

Previous Master theses projects conducted in collaboration with Azelio addressed a similar task [Lantz, 2020] & [Varisco, 2021]. However, potential applications were examined in a broader sense, assuming constant loads and neglecting actual hourly energy demand profiles. Future work recommendations included more accurate modelling and the use of validated assumptions. As a result, the emphasis of this thesis has been on developing a model capable of evaluating promising applications using more precise input data.

The model was developed to serve as an intermediary tool between business development and the engineering department to analyze the technical suitability of the TES.POD using accurate demand profiles and evaluating the investment using data from the investigated application's existing energy system. The main objective is to provide a preliminary result and insight into the investment suitability of TES.POD in a number of potential industrial applications.

Part I. Theory

This part provides an overview of the theory of energy storage systems and explains the current global energy storage market in terms of heat and electricity storage.

3. Energy storage

Increasing political and societal incentives as well as low operating costs will most likely lead to an increased share of renewables in the electricity system. Higher shares of renewable power sources will transform the power grid from a traditional centralized energy system with few large-scale power plants to a more distributed energy system. This development will be challenging because existing systems are generally designed to generate power at transmission level and deliver it at distribution level. However, renewable power generation plants are generally smaller and operate mostly at distribution level [McIlwaine et al., 2021].

This has advantages because more locally generated power reduces distances between producer and consumer, thus, reduces the need of costly transmission lines. However, the increasing penetration of renewable power will bring variability and uncertainty into the electricity system [Göransson]. While small amounts of renewable energies can be easily integrated, larger installed capacities puts the electricity system at risks [Bauknecht and Brunekreeft, 2008]. This limits the cost-competitiveness of renewables and, thus, hinders the transition to a 100 % renewable energy system. To avoid this, flexibility measures which counteract these issues must be introduced.

Energy storage is one promising solution addressing these issues. By balancing mismatches between energy production and consumption, frequency control is introduced, curtailment can be avoided and cost-competitiveness of renewables over thermal power plants is enhanced. Therefore, energy storage technologies are expected to gain increasingly in importance [LDES Council, 2022].

3.1. Energy storage principle

In following, the principle of function of energy storage is explained.

Energy is required whenever some type of 'action', or physically speaking, work, is carried out. Work is not done on a constant basis and the demand for energy differs over time.

Energy demand profiles follow daily- and seasonal variations. In general, energy demand is higher during the day than at night. In countries located in colder climates, heating demand increases during the winter months. In traditional energy systems, energy supply technologies are categorized into base-load and peak-load technologies. Base-load power plants are characterized by large capacities, high investment cost but low operational costs. These technologies have high full load hours and supply the fixed part of the demand which is mostly constant throughout the day and season. Coal-fired power plants and nuclear power plants are considered as typical base-load technologies.

For certain hours during the day or certain time periods during the year, demand exceeds that of the remaining hours. In order to cope with the increased demand, power plants with the capability to deliver a lot of power in a short time are needed. These technologies are called peak-load technologies. They are characterized by relatively low investment costs and high operational costs due to high fuel costs. Thus, they only operate when needed and impose high electricity prices when in operation. Gas turbines, running on natural gas, are a typical peak-load technology.

Renewable power plants cannot be categorized in a traditional way. Their power output is dependent on weather conditions and not on fuel. Depending on the installed capacity and time, renewable power can supply base-load as well as peak-load demand. This can be problematic for the power system because imbalances between power supply and demand can occur more often and be more severe. High shares of renewables generating cheap electricity can displace the need for power produced from costlier technologies or force them to operate on a cyclical basis. However, inflexible power plants, such as coal and nuclear, are not designed for that purpose and often cannot afford to stop operating due to high start-up costs and long ramp-up times. At times of high solar and wind power generation, oversupply can occur because traditional base-load power plants continue operating [Gonzalez-Salazar et al., 2018].

The figures 2 and 3 depict the Spanish energy system for a summer and winter week in 2015, respectively. The shares of power-supplying technologies in the energy system are illustrated as stapled areas under the red coloured supply curve. The load demand is shown as a blue line. The data comes from the Spanish Transmission Service Operator (TSO) [ENTSOE]. Solar and wind power are depicted as yellow and black colored areas, respectively.

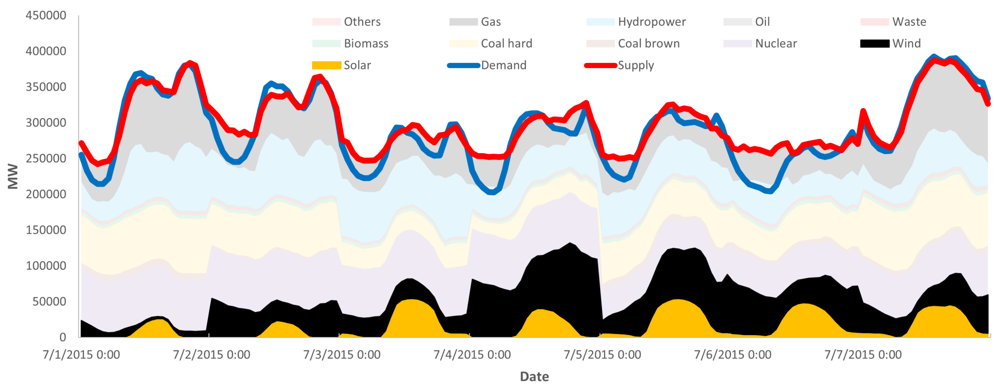

Figure 2: Energy demand and supply profile of Spain for a summer week in 2018 [ENTSOE]

The figures illustrate the problem that can occur if high capacities of renewable power exist in the energy system, such as those present in Spain. For certain

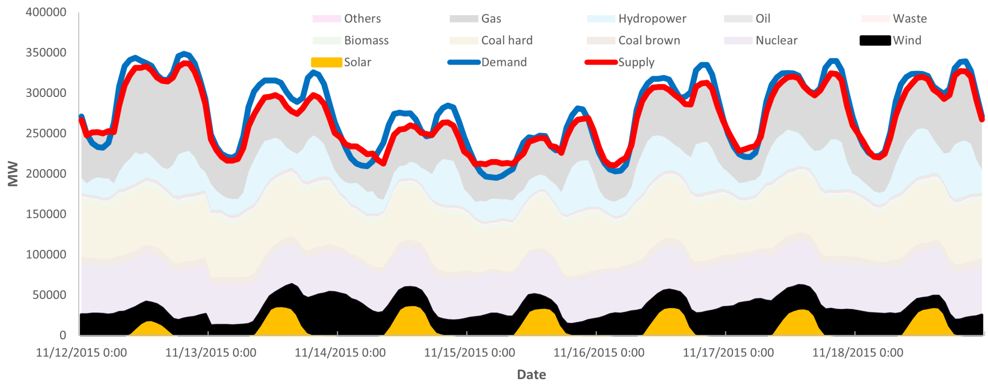

Figure 3: Energy demand and supply profile of Spain for a winter week in 2018 [ENTSOE]

hours during the summer week in figure 2, power supply exceeds load demand, especially between day four and seven, where wind and solar power, colored in black and yellow, rise in value. Solar and wind power generation peaks at around 30 GW on day one and 130 GW on day four. However, inflexible technologies, such as coal, oil, and nuclear power, remain relatively steady throughout the week. The coefficient of variation, a measurement to compare variation between data, illustrates the inflexibility of these technologies. While coal, oil, and nuclear power have a value of 20 %, solar and wind power vary with a value of 55 %. During hours of low demand and high renewable power output, large amounts of power are curtailed due to the inability of base-load technologies to reduce supply, either for technical or monetary reasons.

On the other hand, figure 3 shows the problem that can occur if renewables have a very low power output. During the winter week, the peak power output of solar and wind power combined is at around 60 GW. The coefficient of variation for coal and nuclear power is at 8 % indicating that these technologies are operating at maximal capacity. However, due to the low power output of solar and wind power, the energy system is often not capable of meeting the demand.

Increased use of renewables would exacerbate the supply-demand problem. This is bad for the energy system because differences between supply and demand lead to frequency variation of the AC current, which at certain levels can damage generators and power electronics.

Flexibility measures such as energy storage systems can help the electricity system to maintain acceptable levels of balance between supply and demand in the system. At times of oversupply, storage technologies absorb and store the excess energy. The energy is dispatched if demand exceeds supply in the system.

Energy systems with high shares of renewables highly benefit from energy storage systems. As can be seen in figure 4, oversupplied renewable energy colored in green is prevented from curtailment by using it to charge the storage system. At times of supply deficit, colored orange, energy from the storage system is discharged. Hence, energy storage brings the energy system into balance and so avoids the need for costlier fossil fuels as back-up power [Palmer and Floyd, 2020].

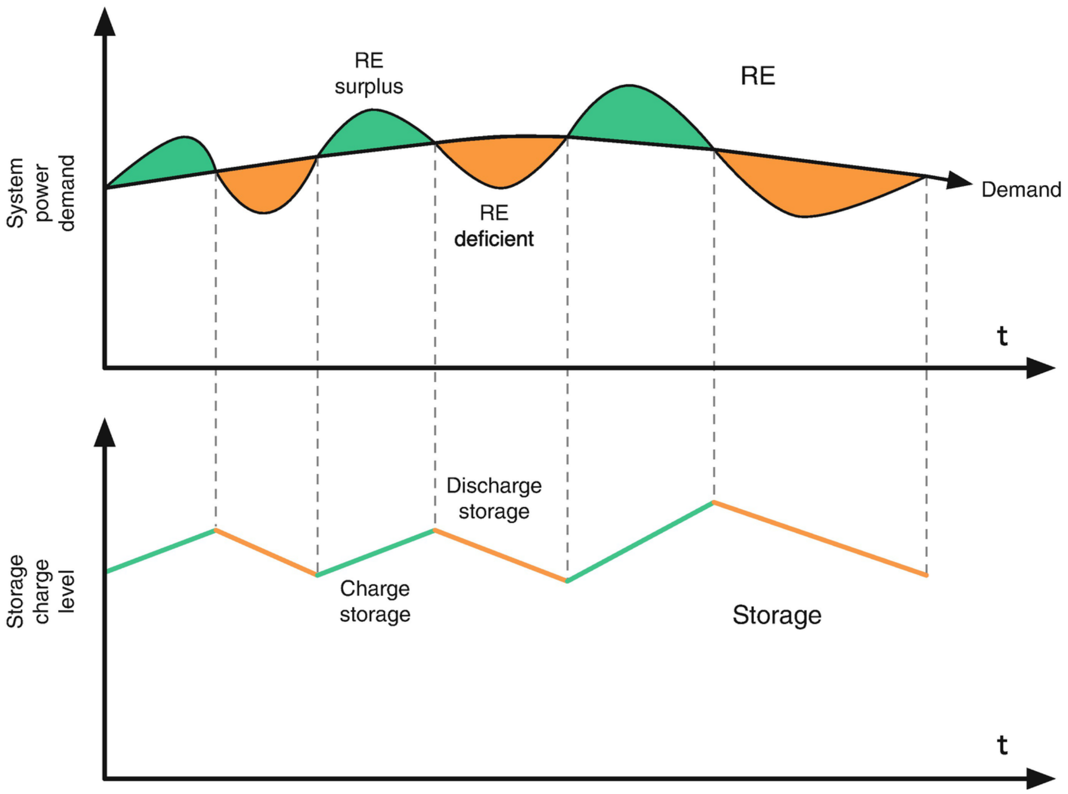

Figure 4: Energy storage principle [Palmer and Floyd, 2020]

3.2. Energy storage market

According to the 2021 World Energy Outlook from IEA [a], renewable energy sources have been the most resilient against Covid-19 lockdown measures. This is attributed to completion of new wind & solar projects and depressed electricity demand. Wind and Solar power plants tend to have lower operational cost and are therefore dispatched first before other power generation technologies. Meanwhile electricity generation from fossil-fuel power plants fell to a 20-year low. Wind & solar power established itself as the cheapest source for electricity and with policy support in over 130 countries, capacity from these power sources are expected to grow faster than other sources [IEA, a]. With that, services which can provide flexibility, such as energy storage, are likely to grow likewise.

Increased capacities of renewable power sources stimulated growth in battery storage capacity by 5 GW in 2020. That is a 50 % increase since 2019. Utility scale installations account for 2/3 of total added capacity. The majority of added capacity of 1.5 GW and 1.6 GW is accounted to the United States and China. IEA [d] estimates that in order to reach Net Zero Emissions by 2050, battery storage capacities need to increase up to 585 GW by 2030. This is, as can be seen in figure 5, a very big leap from current levels of around 17 GW in 2020.

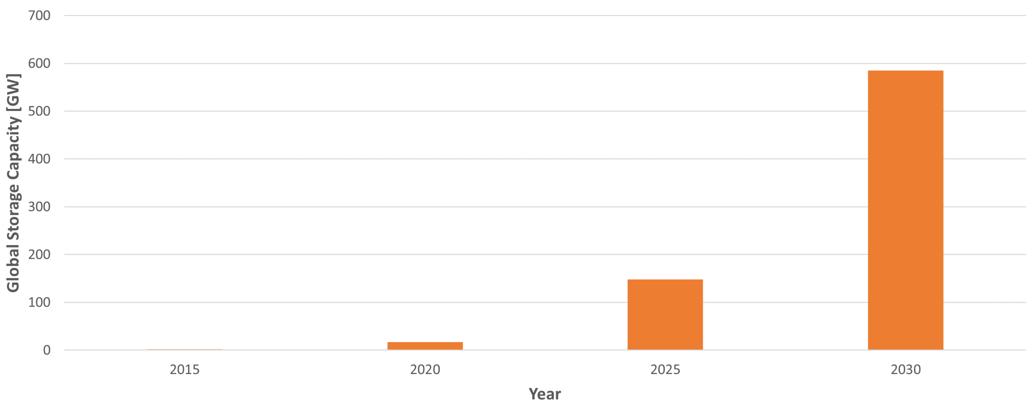

Figure 5: Global energy storage outlook to reach Net zero emissions by 2050 [IEA, d]

China recently announced plans to install more than 30 GW by 2025, excluding pumped hydropower. The United States Congress approved a 900 billion USD

Covid-19 relief bill which includes a two-year extension of the solar investment tax credit (ITC). The ITC is a 26 % tax credit on solar systems on residential and commercial properties. It includes energy storage investments tied to the solar system. The 2020 extension provides market certainty for companies which develop long-term investments [SEIA, Solar Energy Industries Association].

In Germany residential and commercial installations nearly doubled and in October 2020, the United Kingdom's National Grid Electricity System Operator launched a Dynamic Containment frequency response service. It is aimed to stabilize frequency in the system by contracting providers which can provide electricity below sub -one second response time. This is considered as a great opportunity for battery storage providers.

As of 2020, the market for newly added energy storage capacity is vastly dominated by Lithium-ion battery storage systems with 93 % market share [IEA, d].

Considering that battery technologies can only fulfill a certain range of service applications but energy storage applications vastly differ in capacity, power and duration, it can be concluded that other types of storage system can be expected to appear on the market. The outlook for the energy storage market looks promising and significant amounts of growth for all types of storage systems are to be expected.

3.2.1. Thermal energy storage & Heat sector

The focal point of this thesis is the energy storage technology from Azelio AB and the utilization of the heat rejected from the Stirling engine unit during power generation. Thus, a more detailed focus is placed on Thermal Heat storage technologies and the heat energy sector.

In the domestic sector, heat accounts for 70-80 % of the final energy end-use, mostly for water and space heating [SAD, 2022]. In Europe, half of energy consumption for buildings and industry is related to heating and cooling. The demand for heat is higher than for cooling, but the EU estimates that by 2023 the cooling demand will increase by 72 % whereas heating demand in buildings will fall by 30 %. By 2060 energy usage for cooling purposes is expected to overtake that used for heating [IRENA, International Renewable Energy Agency, a].

According to the 2021 outlook of the Thermal Energy Storage Market Research Report [TES, 2021], the TES sector is expected to grow from 4 to 7 billion euros by the end of 2025. This corresponds to a 74 % increase.

3.3. Classification of Energy storage technologies

All the existing energy storage technologies have in common the ability to store energy over a certain time period. However,these technologies differ in response time, storage duration and discharge capacity. Depending on the type of application, different types of services are required. These include:

- Frequency regulation services. Providing grid support by maintaining frequency caused by imbalances between supply and demand.
- Contingency reserve. Providing power reserves for a certain time period.
- Voltage support. Providing or absorbing reactive power to help maintain local voltage levels.
- Black start capabilities. Providing sufficient power capacities at shutdown conditions, without needing grid support.

Energy storage has the potential to improve power quality and reliability. However, power grid issues can range from rapidly changing, unpredictable imbalances to long-term, seasonal variations. A variety of energy storage systems, providing grid services at all levels, are required to improve grid quality across all levels of the electricity supply chain [CTCN, UN Climate Technology Centre & Network].

In following, the major energy storage market players are presented by technology class.

3.3.1. Mechanical energy storage

Mechanical storage technologies include Flywheels, Compressed air storage technology and pumped hydropower storage. Pumped hydropower storage accounts globally for the highest installed energy storage capacity of 153 GW [McIlwaine et al., 2021]. In 2018, out of the 25.2 GW installed energy storage capacity in the United States, 94 % was pumped hydro storage, see Figure 6.

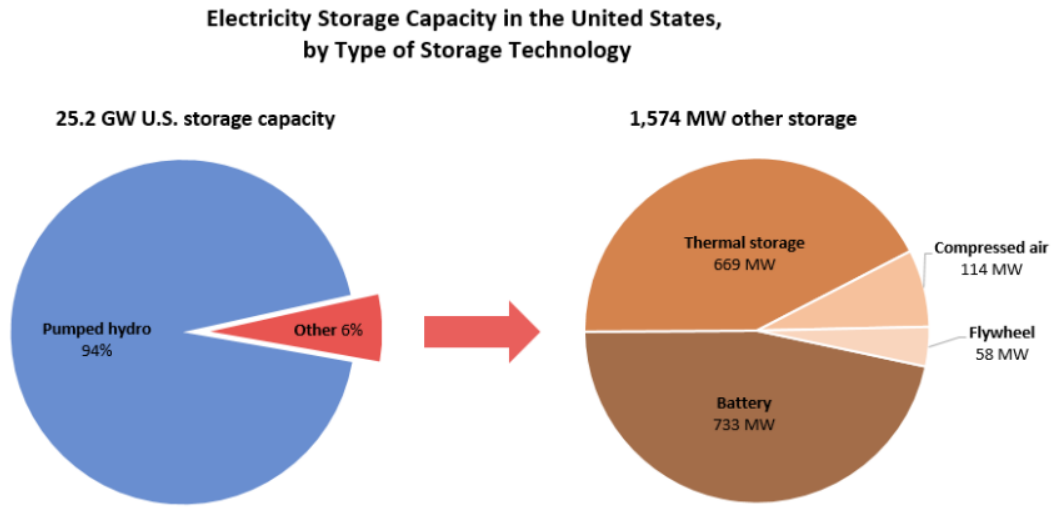

Figure 6: Electricity storage capacity in the United States, by type of storage technology, 2018 EPA, United States Environmental Protection Agency

It can provide a variety of energy system services, such as back-up power and peak-shaving but it is geographically limited, environmentally concerning and capital-intensive [McIlwaine et al., 2021].

3.3.2. Electro-chemical energy storage

Electro-chemical storage technologies hold and release energy through chemical reactions which causes electron transfer through a wire. Batteries are the most common electro-chemical applications.

A battery consists mainly of two electrodes which are connected via a wire and physically separated by an ion-conducting electrolyte. By receiving or producing electricity, the battery performs oxidation and reduction processes. This releases ions moving through the electrolyte from one electrode to the other while simultaneously electrons move through the wire. Batteries are mostly classified on the basis of their active material engaging in these reaction processes. Examples include zinc-bromine, lead-acid and nickel-cadmium batteries. Lithium-ion batteries have emerged as the most promising technology, having a wide range of applications from portable devices to large grid applications. They are characterized by having high energy density and a long life-time, as well as being lightweight and efficient. However, depending on their size and application, they can be temperature-sensitive [McIlwaine et al., 2021]. Some key materials in Lithium-ion batteries are highly toxic, rare, environmentally concerning and involve highly dubious supply chains. For example, cobalt comes mostly from the Democratic Republic of Congo where mining conditions are connected with severe human rights issues. Lithium deposits are mostly located in Argentina, Bolivia and Chile. Increasing demand raises questions about resource security.

Double-layered supercapacitors are promising electro-chemical storage systems that can generate extremely high levels of power without any of the degradation issues that batteries have. The storage capacity exceeds that of a conventional capacitor by replacing the dielectric medium, separating the two charged conducting plates, with an electrolyte. As both conducting plates are charged and charge carriers are separated, ions in the electrolyte arrange themselves towards the plates and thus add capacitance to the system. The technology is able to release high amounts of power significantly faster than batteries but is characterized with a lower energy storage capability [Sinha and Kar, 2020].

3.3.3. Chemical energy storage

Biomass and fossil fuels, such as mineral oil and natural gas, are energy carriers themselves. In the case of fossil fuel, high quantities of energy are stored and thus, by combusting them humans are able to supply large quantities of their energy demand. The three main elements in the chemical energy industry are Carbon, Hydrogen, and Oxygen. These elements are present in biomass as sugar $C_6H_{12}O6$ and in hydrocarbons, such as methane, gasoline, diesel and kerosene [Kauranen et al., 1991]. However, the combustion of these materials results in CO_2 emissions. Hence energy carriers such as Hydrogen are increasingly gaining attention as an alternative because the combustion of it only produces water. Hydrogen can be produced by splitting water with clean generated electricity and combusted or used in fuel cells in the transport and energy industry [Breeze, 2018].

Hydrogen as an energy carrier and so as an energy storage medium is interesting as it is the most abundant material in the universe and has the highest energy density out of all gases. However, it is very low in volumetric density and is energy intensive to produce. [Kauranen et al., 1991].

3.3.4. Comparison of energy storage

Figure 7 illustrates an overview of various energy storage technologies and their capabilities differentiated by start-up time, duration and discharge capacity.

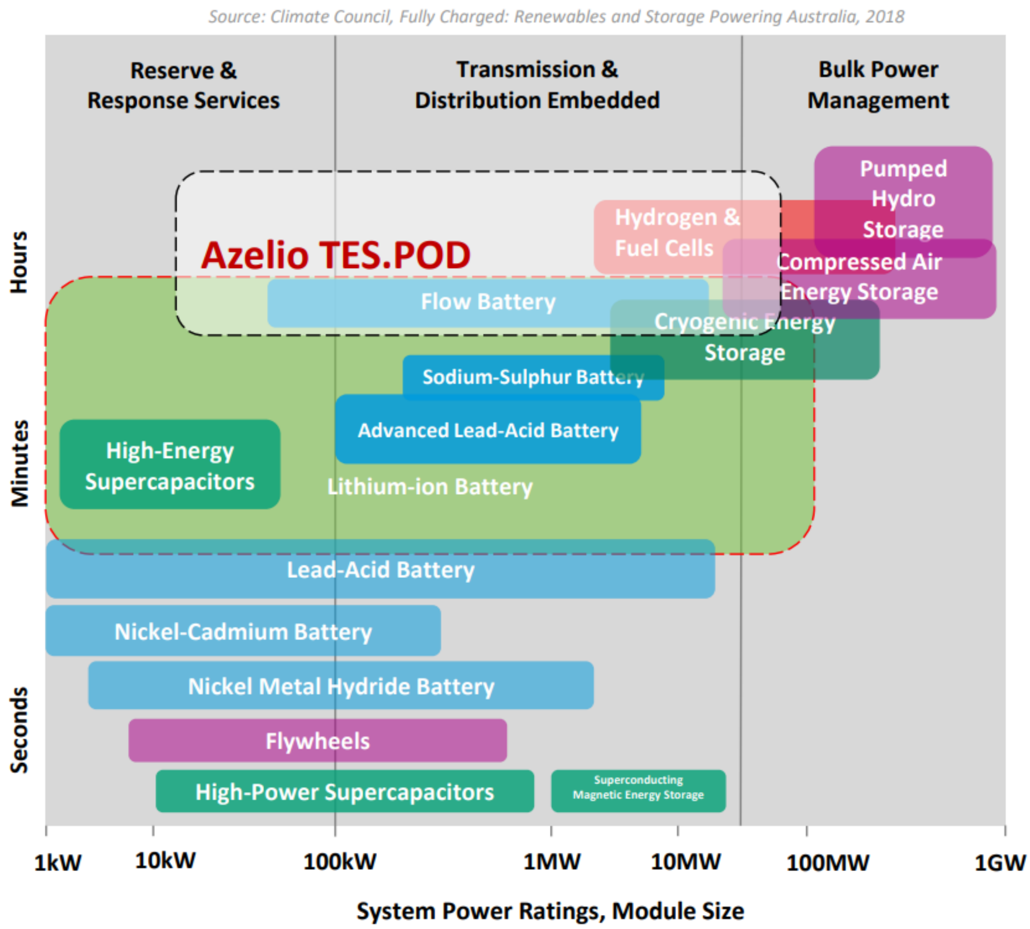

Figure 7: Energy storage technologies, including the TES.POD, and their classification by response time/duration and power capacity. [Engevity, 2021]

At the far end of the figure, Compressed air-, and pumped hydro storage dominate the high duration and high capacity market. These technologies have black-start capability but are inflexible at lower power levels and have slow ramp-up times.

At the other end of the spectrum, lie super fast responding power technologies such as Supercapacitors, which can provide quick high-power services in case of interruptions with duration less than two seconds. However, the drawback of these technologies is that they are limited in discharge duration capabilities.

In between these two extremes, a variety of storage technologies exist which can provide mid to long duration power, with relatively quick responding times. Lithium-ion batteries cover the biggest area, able to provide fast response time services to hourly duration across a large range of capacity. The TES.POD is located above the Lithium-ion battery, slightly overlapping with the battery. It can provide longer duration services but is more limited in response time and range in capacity.

3.4. Carnot batteries

The TES.POD can be categorized as a Carnot battery which can be defined as an Electrical Energy Storage system storing electricity as thermal energy in a storage medium [Dumont et al., 2020]. Hence, the working principle of Carnot batteries and of the TES.POD are explained below.

Carnot batteries are characterized by primarily having an electrical input, and -output. Besides electricity, useful energy outputs can include thermal energy flows.

Carnot batteries can be divided into subgroups depending on which heat storage technology is used. Heat storage can be sensible, latent, thermochemical or a combination of multiple configurations. Latent heat storage systems have a storage medium which undergoes phase-changing while charging. This is beneficial because phase-changing materials absorb or release latent heat at constant temperatures. Latent heat storage systems are associated with higher specific energies $50 - 150\frac{W_{th}h}{kg}$ [Lantz, 2020].

According to McTigue [2019], Carnot batteries have some advantageous properties over other current storage technologies. The technology is not limited by geographical constraints and is modular. Contrary to other storage technologies such as Lithium-ion batteries, Carnot batteries can use non-toxic, cheap, abundant materials for their storage medium.

3.4.1. Working principle

The charging process is the first step which includes the transformation of electricity to heat. Input electricity completes work by creating a temperature difference between two environments. In accordance with the laws of thermodynamics, work is required to create a heat flow from a low to high temperature reservoir. The work spent in this process is stored as thermal exergy. In the discharge step, the thermal flow is allowed to flow with the thermal gradient from the high temperature- to low temperature reservoir. A heat engine in the system converts the streaming heat into electrical work. The remaining heat flows to the low temperature reservoir. The efficiency of the process increases with a greater temperature difference between both reservoirs. The charging process can be achieved using heat pumps or direct resistance heating. Various thermodynamic cycles, including Stirling, Rankine and Brayton can be used as heat engines in the discharge process [Lantz, 2020].

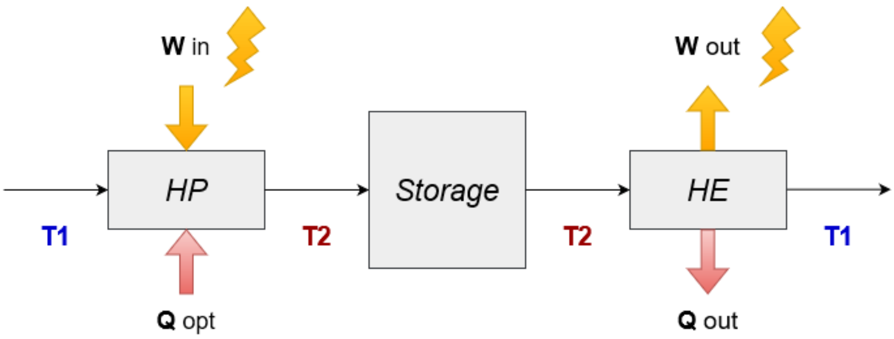

Figure 8: Schematic of Carnot battery

Figure 8 shows a simplified illustration of the Carnot battery process. HP stands for Heat Pump, which uses work W_{in} in form of electricity to elevate temperatures from temperature level $T1$ to $T2$. Optionally, a heat flow Q_{opt} can be integrated to increase the temperature difference. In the storage unit $Storage$, the elevated heat remains in the high temperature level $T2$. When discharged, heat from $T2$ flows into $T1$ while a heat engine HE converts part of the heat to electricity W_{out}. The remaining energy is discharged from the engine as excess heat Q_{out}.

3.4.2. Azelio's TES.POD

Azelio's thermal heat storage system uses Carnot battery technology based on a latent storage medium. The phase-changing storage medium (PCM) is an alloy made out of recycled aluminum and the heat engine converting heat to electricity is a Stirling engine. While charging, electrical resistance is used to heat up the PCM up to 600 °C. It changes phase from solid to liquid. Electricity discharge occurs when the PCM transfers heat through a heat transfer fluid to the Stirling engine. Inside the Stirling engine, a working gas is heated by the fluid and thus drives the two pistons inside the engine. This process creates the momentum to drive the generator. Figure 9 illustrates the schematic of the Stirling engine and the cooling system. A coolant radiator uses incoming air to cool down a water cycle. The working gas and cooling oil for the lubricant and cylinders is cooled down through two separate heat exchangers connected to the water cycle. The water loop contains about 50 % glycol. The temperature entering the radiator is flexible but set to a max. temperature at around 70 °C. The temperature difference over the radiator is 7.5 °C.

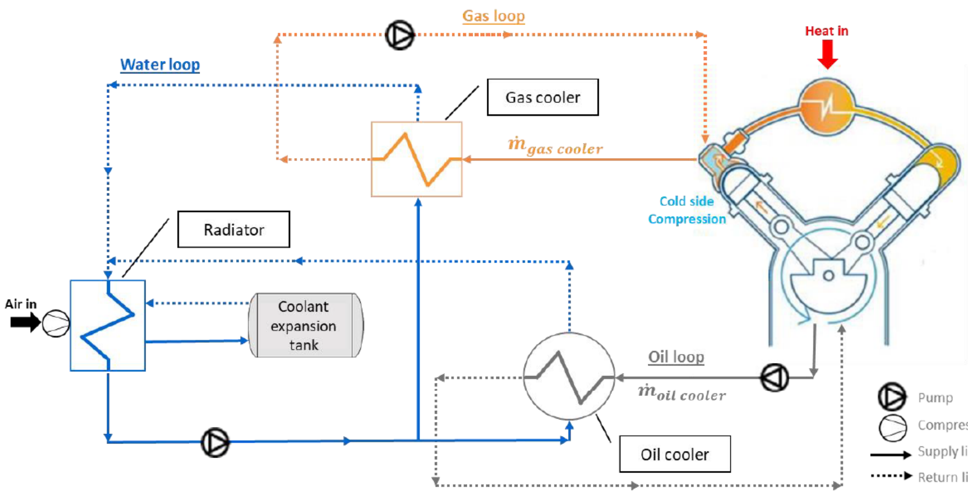

Figure 9: Schematic of Stirling engine and cooling system

The system is scalable which means multiple TES.POD units can be connected in parallel and charged/discharged at the same time. The estimated lifetime of the TES.POD is 30 years. One unit takes 6 h to fully charge, with a maximum charging power of 100 kW. This amounts to 600 kWh energy capacity. Electricity discharges at a maximum output of 13 kW and under continuous operation 12.1 kW. The TES.POD can discharge for up to 13 h. Under these conditions, the electrical energy output corresponds to 157.3 - 169 kWh. During discharge, the heat released by the Stirling engine corresponds to around two thirds of the initial energy input.

In order to utilize the heat and hence, run the TES.POD in Combined Heat and Power (CHP) configuration, the cooling system and the cooling radiator running on air is either kept for drying applications or replaced by a liquid-liquid Heat exchanger configuration running on water. As can be seen in figure 10, such a configuration is used to replace the cooling radiator seen in figure 9.

Depending on the cooling water temperature entering the heat exchanger, additional heat in the form of water could be provided with temperatures up to 65 °C.

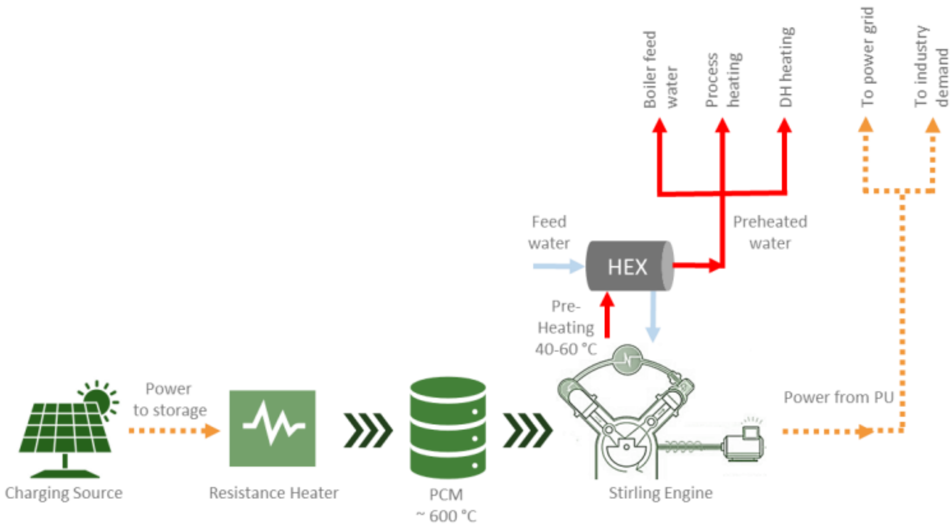

Figure 10: Schematic of TES.POD operating in CHP mode

With multiple TES.POD's in the system, one configuration could be a single HEX connected to the different Stirling engine units, as can be seen in figure 11.

The scalability of the TES.POD allows to match customers in a variety of sectors and to cover a wide range of demand. Around 80 units of the TES.POD can provide

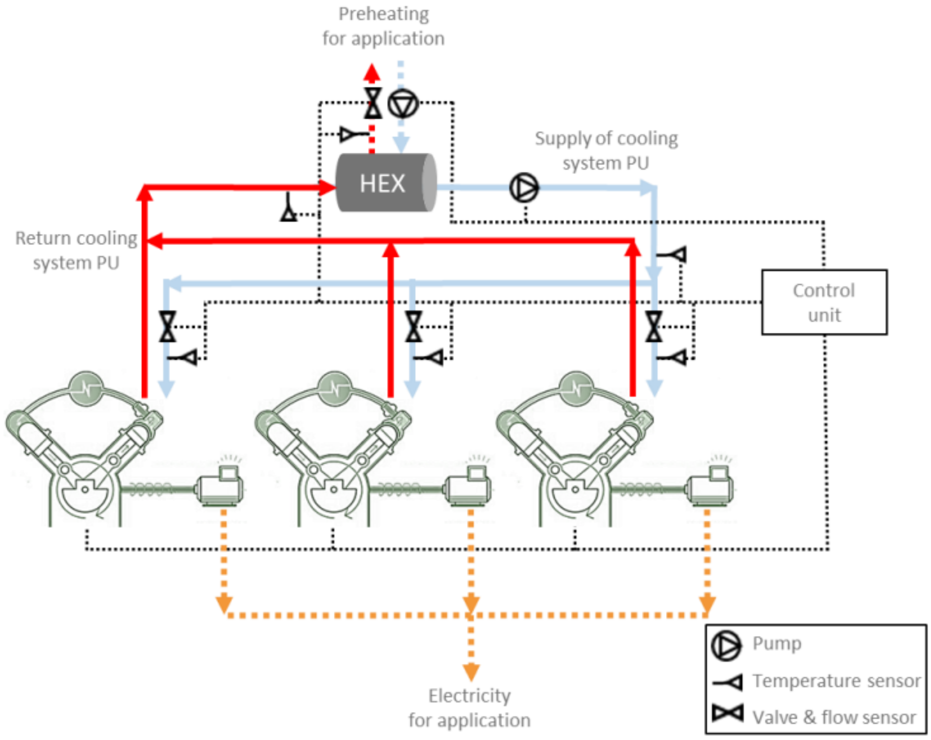

Figure 11: Schematic of HEX configuration with multiple TES.POD's

more than 1 MW of electrical power and 2.4 MW thermal power, assuming rated power. The unit discharge capacity corresponds to 13.5 MWh_{el} & 31.3 MWh_{th}, assuming 13 hours of duration at rated power. Table 1 lists the relevant technical values.

Technical properties	Value	Unit
Max charging power	100	kW_{el}
Charge duration at max	6	h
Discharge duration at max	13	h
Nominal el. Power output	13	kW_{el}
Continuous operating el. power output	11 - 12.1	kW_{el}
Nominal thermal power output	30	kW_{th}
Continuous operating output	26	kW_{th}
Rated el. energy capacity	165	kWh_{el}
Rated thermal energy capacity	385	kWh_{th}
Rated total energy capacity	550	kWh_{th}
Lifetime	30	years

Table 1: Technical properties of the TES.POD

3.5. Lithium - ion batteries

Globally, battery storage technology is quickly expanding, with lithium-ion batteries emerging as the most promising technology. [IEA, d]. As can be seen in figure 7, the technology competes with the TES.POD by providing a similar range of power capacity and discharge duration. As a result, if not considered complementary, it can be considered the main competitor to the TES.POD in the market. They are similarly modular and scalable, but outperform the TES.POD in terms of efficiency, as well as flexibility, due to very short start-up times. Although capable of providing power for longer duration periods, they are disadvantageous for longer than 2 - 4 hours [Goldstein, 2021]. Furthermore lithium-ion batteries have a shorter lifetime of max 15 - 20 years. However this is dependant on the operating conditions. The number of charge and discharge cycles a battery can operate is limited and affected by the operating Depth of Discharge (DOD) which is a percentage based on the ratio of operating- to rated capacity. Operating the battery at higher rates of DOD reduces the number of cycles.

Part II. Methodology

Azelio has previously investigated potential market sectors where the TES.POD is most promising for adding flexibility to the power system. These include: Communities & Societies, Commercial Facilities, Agriculture, Desalination and the Mining industry. These sectors require stable power for longer periods of time and are commonly located in remote areas with limited or no access to the power grid. As a result, these industries have an economic incentive to use renewable energy in conjunction with the TES.POD to deliver cheap, reliable electricity.

However, only a limited amount of research has been done on potential markets for the heat generated by the TES.POD. To investigate potential applications for the TES.POD in CHP configuration, the suitability and profitability of the storage system in the respective energy system needs to be checked.

This chapter presents the working procedure and the methodology of the techno-economic analysis. The working procedure includes the identification, analysis, and evaluation of potential applications.

The analysis is done by constructing a mathematical model which can deliver an economic evaluation of any kind of electric energy storage system. The aim of the thesis is the analysis and evaluation of the value of the excess heat released from the TES.POD while it is discharging electricity, thus, the model includes the analysis of the heat generated while in operation. The model can thus be used to compare the techno-economic performance of different energy storage technologies for a specific application.

4. Working procedure

Figure 12 shows the working procedure of identifying, analyzing, and evaluating potential applications. The procedure is subdivided into three parts:

- Identification of promising applications

- Fundamental analysis
- Sensitivity analysis

The procedure is performed step-wise as indicated with arrows in between each process.

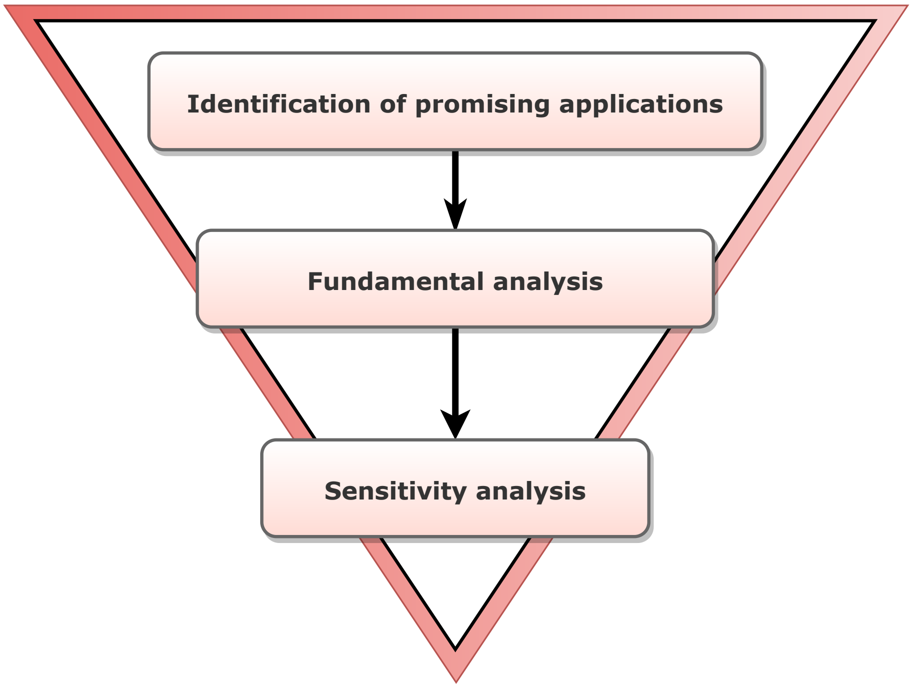

Figure 12: Flow chart of working procedure

4.1. Identification of promising applications

In order to analyze and evaluate potential applications, they need to be identified in the first place. Based on literature research, knowledge about a variety of industries is collected. These industries were screened to find suitable applications where the TES.POD as a CHP unit, providing electricity and heat, could potentially be integrated. In order to successfully identify an application within an industry, 4 key criteria need to be fulfilled, as seen in figure 13.

1. criterion

Although the TES.POD can provide flexibility to various renewables, such as wind power, the analysis conducted in this thesis is constrained by using solely solar power. Based on the application's energy system, the model calculates the required solar power capacity, to meet the electricity demand, and the energy to fully charge the TES.POD during the day. Solar power, unlike wind power, has a daily power-generating cycle that repeats itself, making it more suitable for the following analysis, which assumes a constant daily power-generating profile.

As solar power is strongly dependent on geographic location, its technical suitability to deliver steady power throughout the year must be met.

2. criterion
The investigation and evaluation of an application's energy system for potential integration of an energy storage technology requires data about the application's electricity demand.

The storage system is assumed to meet the electricity demand during the night when solar power stops generating. Thus, the demand must contain values at night which if not would make the storage technology unnecessary because all the power demanded from the system could be meet by the solar power technology.

3. criterion
In the case of the TES.POD or a similar technology where heat is generated while the technology is providing electricity, an economic value for the heat can only be estimated if the investigated application has a suitable heat demand which the storage technology can meet. Hence, similarly as with in criterion 2, a heat demand profile in hourly resolution for at least 24 hours must be available. If the heat generated by the storage technology is desired to be utilized instantly, the heat demand must reflect energy values bigger than zero during nighttime.

4. criterion
Even if the application has an existing heat demand, the heat generated by the storage technology is of no value if the temperature level of the heat does not match the heat requirements of the application. In the case of the TES.POD, the value of the heat generated is mostly limited by the temperature level of 65 °C. The investigated application must require heat at 65 °C or lower.

If an investigated application does not fulfill all of these criteria, it was discarded for further analysis.

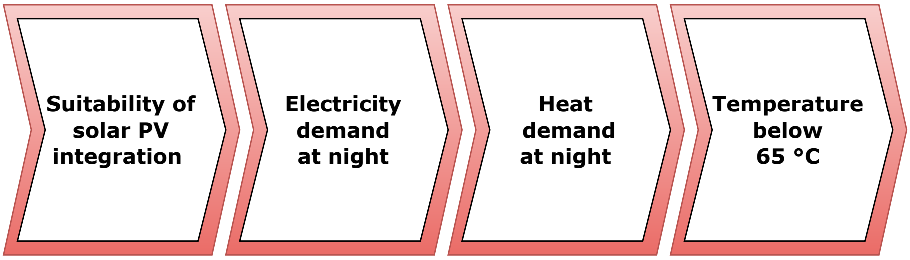

Figure 13: Key criteria for the identification of promising applications

4.2. Fundamental analysis

After identifying potential applications, fundamental thermodynamic and economic calculations are conducted by means of a simplified model of the investigated energy system. The model returns performance indicators which allow for a brief evaluation of whether the investment in the energy storage technology, such as the TES.POD, is profitable. A detailed description of the modelling can be found in Section 5. Furthermore, applying the model with various competing energy storage technologies results in a better insight of the cost-competitiveness of the product.

4.3. Sensitivity Analysis

In the sensitivity analysis, data and techno-economic properties related to the industry and the storage technologies are varied. Future uncertainties and scenarios related to the techno-economic data and fuel prices are tested. The sensitivity analysis allows for a more complete evaluation because the applied model in Section 4.2 only analyzes a static system system with fixed input data.

After this step, the concluding result of the application is presented.

5. Modelling

Figure 14 illustrates an overview of the modelling procedure. The model is constructed using data of various data blocks, coloured in blue. Specific input data to these data blocks is depicted as arrows pointing towards the blue boxes. The resulting green box represents the output of the model, which is a Net Present Value Calculation of the storage technology investment. Hereafter, the modelling is described step-wise.

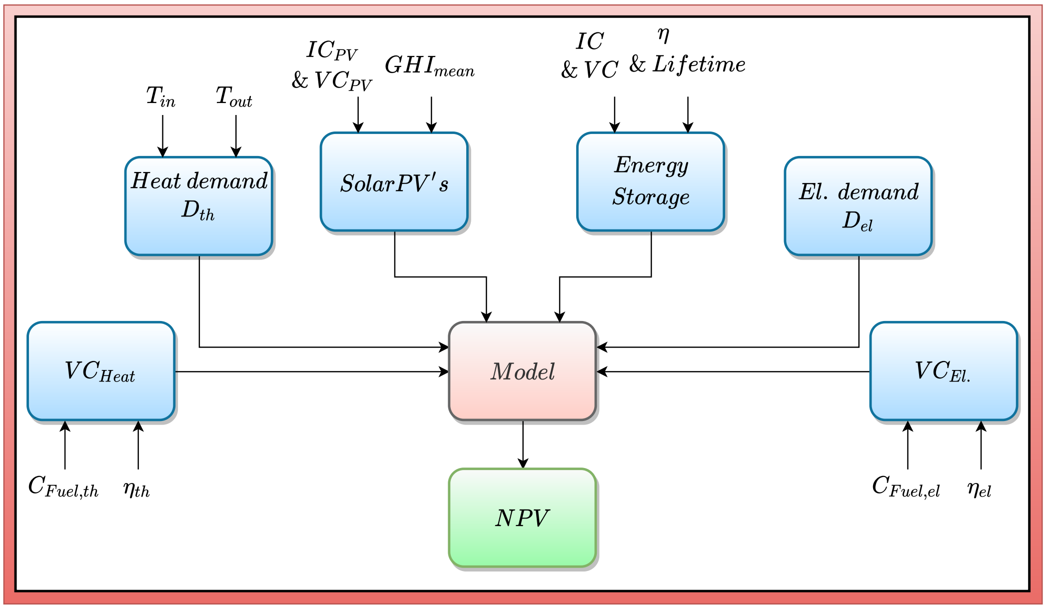

Figure 14: Overview of Modelling

Step 1 - Data collection

As figure 14 indicates, input data is needed in order to construct the model. Table 2 gives an overview of the data that must be obtained beforehand.

Table 2 includes the energy demand profiles of the application's existing energy system, here symbolized as $D_{i,t}$.

$$D_{i,t}, \; \forall_{i,t \, \epsilon \, I,T}$$

Index I stands for the respective energy carrier, being either heat or electricity and index T depicts the time dependency of the energy demand. In the following

Parameter	Description	Unit
$D_{i,t}$	Time dependant energy demand	kW
T_{in}	Hot water supply temperature of application	K
T_{out}	Hot water return temperature of application	K
IC	Capital Cost of storage technology	$\frac{USD}{Unit}/\frac{USD}{kW}$
IC_{Tank}	Capital cost of hot water tank	$\frac{USD}{litre}$
VC	Variable cost of storage technology	$\frac{USD}{kWh}$
η	Electrical efficiency of storage technology	%
$C_{Fuel,i}$	Fuel cost of existing energy generating technology of the respective energy carrier	$\frac{USD}{MWh}$
η_i	Efficiency of existing energy generating technology	%
IC_{PV}	Capital Cost of PV system	$\frac{USD}{kW}$
VC_{PV}	Variable Cost of PV system	$\frac{USD}{kW}$
$Lifetime$	Lifetime of energy storage technology	/
GHI_{mean}	Average solar irradiation value	$\frac{kWh}{m^2}$

Table 2: Input data table

an hourly resolution is used. Ultimately, resulting in a list of energy values for a daily time period.

$$I : [el, th]$$
$$T : [0, ..., 23]$$

Besides the heat demand profile, extra data of hot water supply and return temperatures T_{in} & T_{out} are required.

Data for each investigated storage technology includes the electrical efficiency η, investment cost IC, as well as the variable cost VC.

The expected lifetime $Lifetime$ of an energy storage technology has a major influence on the profitability of a technology and thus, cost competitiveness with other technologies.

Depending on the investigated application and if the investigated ESS provides valuable heat in form of water, such as in the case of the TES.POD, a hot water storage tank could be included. By decoupling the heat demand from the heat generation, the economic value of the ESS could rise. However, this impacts the CAPEX. As a result, capital cost data for the tank IC_{Tank} must be included.

The amount of solar PV's installed is one of the main factors that affects the CAPEX. This amount is affected by the local solar radiation GHI_{mean} and the capital cost IC_{PV} in $\frac{USD}{kW}$.

Furthermore, data about the current energy system, such as fuel costs, $C_{Fuel,i}$, and efficiencies, eta_i, of the currently used energy generating technologies, are required. The model is constrained by the assumption that the investigated application currently meets its electricity and heat demand with a fully operating energy system in place. The monetary evaluation of the storage technology depends on how much the ESS can replace the existing fuel based technologies. Hence, calculations do not include the cost of investment for these technologies. Moreover, the model implies that the existing energy system meets the electricity and heat demand with separate technologies. The model cannot handle application's, generating their energy needs with a CHP technology. Similar to the TES.POD, heat and electricity are generated simultaneously. Replacing electricity generated by the CHP with the ESS and solar PV's affects the ability of the CHP to provide heat.

Step 2 - Base-load electricity demand

Although the TES.POD is technically able to reduce or increase its power output, it is not suitable for very fast changing demand profiles. Considering that the TES.pod operates optimal delivering a constant power output, the TES.POD is assumed to only provide base-load demand during the night.

Based on the electricity demand profile of the application, the base-load demand at night is identified. The investigated energy storage technology will be assumed to be sized to meet the base-load demand throughout those hours. Equations 1 and 2 depict the procedure of finding the minimum value of the electric energy demand for the assumed night period, here indexed with T_N. The resulting value is symbolized as $D_{Baseload,night,el}$.

If no further data is available, the demand profile is assumed to be the same for every day over the investigated time period.

$$T_N : [0, ..., 5], [18, ..., 23] \tag{1}$$

$$D_{Baseload,night,el} = Min(D_{el,t}), \forall_{t \,\epsilon\, T_N} \tag{2}$$

Figure 15 represents an illustrative electricity demand profile for one day. The demand profile is coloured in light blue bars, characterizing the respective hourly power values. The base-load demand at night is depicted as a dark blue shaded area under a black line.

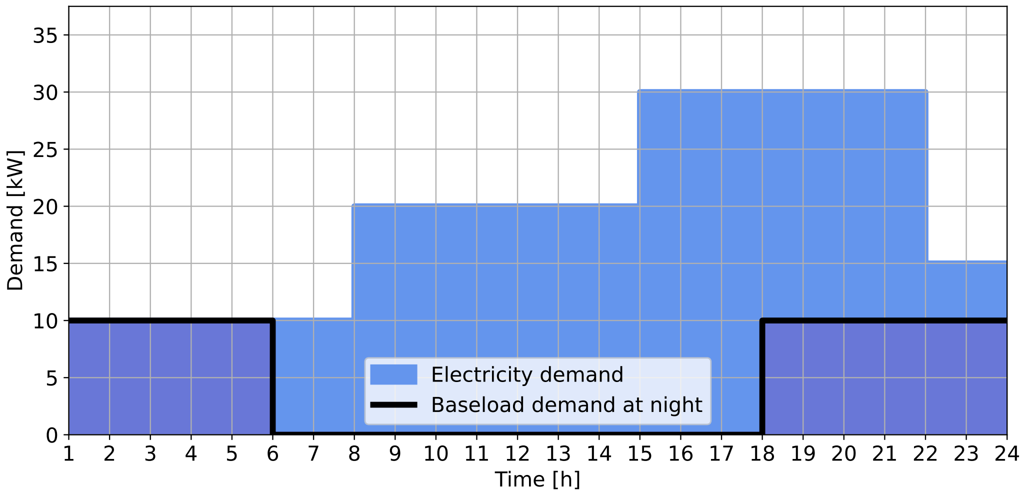

Figure 15: Exemplary electricity demand profile, depicted in light-blue, including the base-load demand at night, depicted in dark-blue under a black line.

Step 3 - Electrical Energy Storage capacity / TES.POD units

The required energy storage discharge capacity $P_{ESS,el}$ corresponds to the base-load power demand at night of the respective energy system, see equation 3. Index ESS stands for Electrical Energy Storage and thus, represents any investigated energy storage technology suitable to provide the power demanded.

In the case of the TES.POD in CHP operation, discharge capacity varies from rated capacity if the TES.pod is required to generate power and heat in useful amounts. Furthermore, because power output decreases with operating time, one TES.POD unit is assumed to provide a constant power output of 10 $\frac{kW_{el}}{TES.POD}$ that is less than the rated power. All the variables related to the TES.POD are represented per unit, thus moving forward the required number of units, $N_{TES.POD}$, must be calculated via equation 4.

$$P_{ESS,el} = D_{Base-load,night,el} \tag{3}$$

$$N_{TES.POD} = \frac{D_{Base-load,night,el}}{10\frac{kW}{TES.POD}} \tag{4}$$

Step 4 - Electricity supplied

Assuming the electricity demand profile does not change throughout the year, the annual electricity discharged by the energy storage system is calculated according to equation 5. It is calculated by multiplying the base-load electricity demand at night $D_{Base-load,night,el}$ with the time of operation (compare Eq. 1). This corresponds to the sum of daily operating hours, multiplied by 365 days. In order to enable a comparison between various storage technologies, the yearly amount of stored and discharged electricity, $E_{ESS,el}$, must be the same for each storage technology.

$$E_{ESS,el} = 365\frac{days}{yr} * \sum_{t=0}^{5}\sum_{t=18}^{24} D_{Base-load,night,el} = D_{Base-load,night,el} * 4380\frac{h}{yr} \tag{5}$$

Step 5 - TES.POD Heat supplied

As previously mentioned, the aim of this thesis is to discover uses and value for the excess heat released by the TES.POD. The amount of heat generated is calculated similarly as in Step 4. The following equations only apply to the TES.POD or similar technologies since for instance, conventional batteries are assumed to not deliver additional energy in the form of heat.

The TES.POD can only provide heat when electricity is generated by discharging the thermal storage. As a result, the amount of heat that the TES.POD can deliver is limited by the time of discharge. As previously stated, power discharge is assumed to only occur at night, between 18:00 and 06:00 (compare Eq. 1).

The generated thermal power from each TES.POD unit is considered to be fixed at a constant value of 22 $\frac{kW}{TES.POD}$. By means of the heat demand profile it is determined if the heat generated by the TES.POD(s) can be supplied to the system. In the event that more heat is generated than demanded, the heat is either curtailed or stored away in a hot water tank for later use.

Equation 6 shows that the total heat generated from the TES.POD cluster $P_{gen,th}$ is calculated, multiplying the number of units with the assumed fixed value of 22 $\frac{kW}{TES.POD}$.

Equation 7 describes that the heat supplied to the system $P_{sup,th,t}$ is always either equal or lower than the heat demand for all hours during times of power output.

As in Step 4, the yearly heat savings are calculated in equation 8 summarizing the supplied heat over the yearly operation time.

$$P_{gen,th} \leq N_{TES.POD} * 22kW_{th} \tag{6}$$

$$P_{sup,th,t} \leq D_{th,t}, \forall_{t \,\epsilon\, T_N} \tag{7}$$

$$E_{ESS,th} = 365\frac{days}{yr} * \sum_{t=0}^{5}\sum_{t=18}^{24} P_{sup,th,t} = 4380\frac{h}{yr} * P_{sup,th,t} \tag{8}$$

As an example, figure 16 illustrates a fictional heat demand profile based on the illustrative electricity demand profile shown in Step 3 (Figure 15), to determine the number of required TES.POD units.

The heat demand is coloured in red. The orange shaded area under the black line is the heat supplied by the TES.POD. If the heat generated by the TES.POD exceeds the actual demand, the remaining TES.POD heat is shown in the colour yellow.

As can be seen, for the hours 20:00 to 04:00, the heat generated by the TES.POD exceeds the demand, while from 04:00 to 06:00 and 18:00 to 20:00, the heat generated by the TES.POD does not. Hence, a hot water tank could be installed.

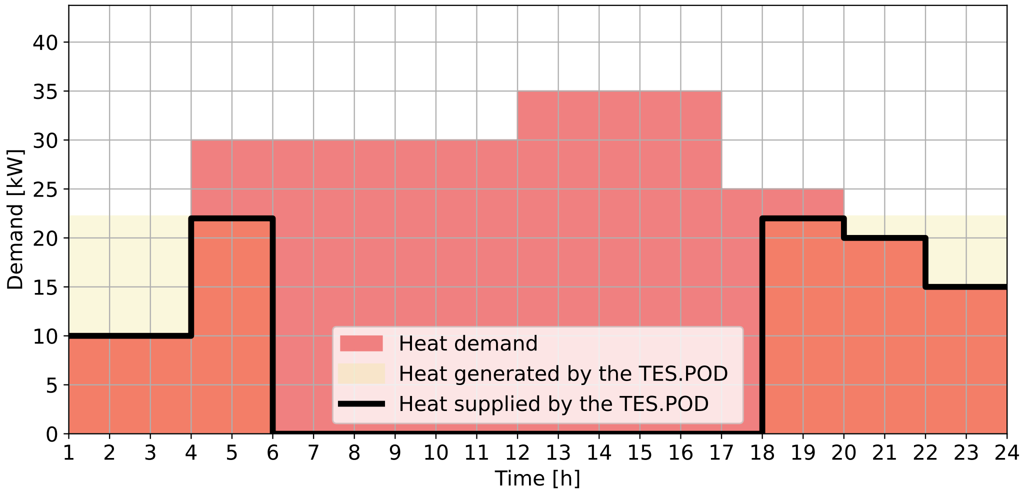

Figure 16: Exemplary heat demand profile depicted in salmon-red, with heat generated and heat supplied by the TES.POD depicted in yellow and orange-red under a black line, respectively.

Step 6 - Hot water tank

If the amount of heat generated by the TES.POD, or similar, exceeds the heat demand during the night, a hot water tank could be included in the system. The otherwise curtailed heat can be used to charge the tank, which in turn can be discharged during the daytime to meet the heat demand. This would further avoid using fuel and thus, generate more fuel cost saving cash flows.

Equation 10 illustrates the calculation of the curtailed heat $P_{curt,th,t}$ which is the heat generated subtracted by the heat supplied from the TES.POD. The annual heat supplied by the tank is denoted by $E_{Tank,th}$.

The sum of the curtailed heat $P_{curt,th,t}$ during the night time determines the total energy capacity of the storage tank Cap_{Tank}.

The current energy stored of the tank is expressed as the State of Charge $SOC_{Tank,t}$ which is modelled in equation 11. The tank undergoes a daily repeating charge- and discharge cycle. Hot water discharge starts when the TES.POD stops operating. Equations 12, 13 and 14 show that the $SOC_{Tank,t}$ at the start of operation corresponds to Cap_{Tank} and that the $SOC_{Tank,t}$ over time decreases depending on the heat discharged $P_{Tank,th,t}$. The heat discharged is equivalent to the heat demand $D_{th,t}$ or the current State of Charge $SOC_{Tank,t}$. The annual energy discharged from the Tank corresponds to the sum of discharged heat $P_{Tank,th,t}$, see equation 15. For simplicity, it was chosen that the hot water tank starts discharging when the TES.POD stops operating, i.e. during day-time.

$$T_D : [6, ..., 18] \tag{9}$$

$$P_{curt,th,t} = P_{gen,th,t} - P_{sup,th,t}, \forall_{t \,\epsilon\, T_N} \tag{10}$$

$$Cap_{Tank} = \sum_{t=0}^{5} \sum_{t=18}^{24} P_{curt,th,t} \tag{11}$$

$$SOC_{Tank,t=6} = Cap_{Tank} \tag{12}$$

$$P_{Tank,th,t} \leq D_{th,t} \cap SOC_{Tank,t} \tag{13}$$

$$SOC_{Tank,t+1} = SOC_{Tank,t} - P_{Tank,th,t}, \forall_{t \,\epsilon\, T_D} \tag{14}$$

$$E_{Tank,th} = 365 * \sum_{t=6}^{17} P_{Tank,th,t} \tag{15}$$

As an example, the same heat profile as in figure 16 is displayed in figure 17 but additionally includes the heat supplied from a hot water storage tank, using the otherwise curtailed heat from the TES.POD. The discharged heat from the tank is depicted in a dark red colour. The figure shows that the curtailed heat, coloured in yellow, is not sufficient enough to meet the whole remaining demand left between 06:00 and 18:00.

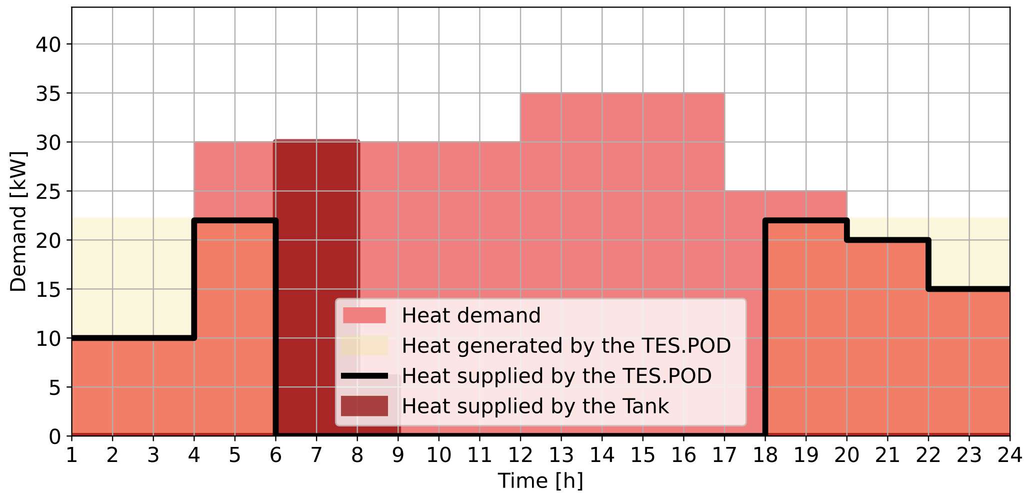

Figure 17: Exemplary heat demand profile depicted in salmon-red, with heat generated and heat supplied by the TES.POD depicted in yellow and orange-red under a black line, respectively. Additional heat provided by including a hot water storage tank using otherwise curtailed heat from the TES.POD is depicted in dark red.

Step 7 - Economic performance of storage system

The CAPEX and OPEX of the storage technology are calculated based on the required capacity or in the case of the TES.POD, the number of units needed $\frac{USD}{TES.POD}$. Azelio has provided company-internal data of capital and variable cost estimates, while for other energy storage technologies cost data can usually be found via literature search. Using capacity based cost estimates in $\frac{USD}{kW}$ requires further calculations using the efficiency η of the technology. In the case of an electric battery, capacity fading must be taken into account [Rudolf and Papastergiou, 2013]. To account for the capacity loss, the initial battery capacity must be oversized to supply the electricity demand even at the end of the lifetime.

Equations 16 and 17 show the calculation steps to obtain the CAPEX and OPEX of the TES.POD technology.

$$CAPEX_{TES.POD} = IC_{TES.POD}\,[\frac{USD}{TES.POD}] * N_{TES.POD} \tag{16}$$

$$OPEX_{TES.POD} = VC_{TES.POD}\,[\frac{USD}{TES.POD * yr}] * N_{TES.POD} \tag{17}$$

Step 8 - CAPEX of HEX & Hot water tank

Depending on the application, one or more heat exchangers are required to extract and deliver the heat generated from the TES.POD. The heat exchanger CAPEX for the TES.POD is either calculated using an internal estimate of Azelio of 1000 $\frac{USD}{TES.POD}$ or via an estimated capital cost target equation 20 for stainless steel shell/tube heat exchangers, according to [Hall et al., 1990]. The equation estimates the capital cost based on the required total heat exchanger area. The heat exchanger area is dependent on the heat produced from the storage technology, the overall heat transfer coefficient, assumed as 1 $\frac{kW}{m^2K}$, and the logarithmic temperature difference between the supply and return water streams, see equation 18 and 19.

Although the equation found in the literature resulted in a significantly higher value than Azelio's estimate, the effect on the model's result was minimal considering that the HEX CAPEX is comparably low to the other CAPEX values.

The CAPEX of the hot water tank is acquired by calculating the required total tank volume in litres, see equation 22. The equation is dependant on the sum of heat delivered during the day from 05:00 to 18:00 and the temperature levels of the hot and cold water streams. The obtained tank capacity determines the CAPEX of the component, see equation 23. By means of literature research the investment cost IC_{Tank} of hot water storage tanks in $\frac{USD}{litres}$ can be found (compare e.g. [Heritage Water Tanks]).

$$\Delta T_{log} = \frac{(T_{Hin} - T_{Cout}) - (T_{Hout} - T_{Cin})}{\ln \frac{T_{Hin} - T_{Cout}}{T_{Hout} - T_{Cin}}} \tag{18}$$

$$Area_{HEX}\,[m^2] = \frac{22\,kW_{th} * TES.POD's}{1000\,\frac{W}{m^2K} * \Delta T_{log}} \tag{19}$$

$$CAPEX_{HEX} = 30800 + 1644 * Area_{HEX}^{0.81} \tag{20}$$

$$T_D : [6, ..., 18] \tag{21}$$

$$m_{Water}[L] = \sum_{t=6}^{T_D} \frac{P_{Tank,th,t}}{4.18\,\frac{kJ}{kgK}(T_{Hin} - T_{Hout})} * \frac{1000\frac{L}{m^3} * 3600\frac{s}{h}}{998\frac{kg}{m^3}}, \forall_{t\,\epsilon\,T_D} \tag{22}$$

$$CAPEX_{Tank} = IC_{Tank} * m_{Water} \tag{23}$$

Step 9 - Economics of solar PV's

Throughout the day, assumed between 06:00 and 18:00, the energy generated by the solar PV's, $E_{el,n}$, must be sufficient to supply the application's electricity demand, $D_{el,t}$, and to fully charge the energy storage technology, see equation 25. The amount of energy needed to fully charge the energy storage technology depends on the storage efficiency η_n of the storage system, i.e. the efficiency describing the losses occurring during the storage period

The required capacity, $P_{PV,n}$, is determined by the required energy, $E_{el,n}$, the peak solar radiation, and the local average Global Horizontal Irradiance (GHI) in $\frac{kWh}{m^2\,day}$, see equation 26 [Nielsen and Thorsteinsson]. Peak solar radiation is globally constant at 1 $\frac{kW}{m^2}$. If no location is specified, the local average GHI can assumed to be constant, e.g., at 4 $\frac{kWh}{m^2\,day}$.

The CAPEX and OPEX values of the solar power system result of the multiplication of the solar power capacity, $P_{PV,n}$, and the chosen capital cost value IC_{PV} and variable cost value VC_{PV}, respectively, see equations 27 and 28.

$$\eta_{TES.POD} = \frac{11kW * 16h}{100kW * 6h} = 29.3\% \tag{24}$$

$$E_{el}\,[\frac{kWh}{day}] = \sum_{t=6}^{17} D_{el,t} + \frac{\sum_{t=0}^{5}\sum_{t=18}^{24} D_{Baseload,night,el}}{\eta} \tag{25}$$

$$P_{PV}\,[kW] = \frac{E_{el} * 1\frac{kW}{m^2}}{GHI_{mean}\,[\frac{kWh}{m^2\,day}]} \tag{26}$$

$$CAPEX_{PV} = P_{PV} * IC_{PV}\,[\frac{USD}{kW}] \tag{27}$$

$$OPEX_{PV} = P_{PV} * VC_{PV}\,[\frac{USD}{kW\;yr}] \tag{28}$$

Step 10 - Fuel cost savings

The cost savings by replacing the existing energy generating technology with heat & electricity, supplied by the investigated storage technology represent the positive cash flows in the NPV calculations presented below.

The variable cost $C_{var,i}$ of producing electricity or heat with the current system is calculated by dividing the fuel cost C_{Fuel} with the efficiency η_i of the existing energy-generating technology, see equation 29. To get the fuel cost savings, the resulting variable cost for electricity and heat must be multiplied with the annual electric and thermal energy delivered from the storage technology. The resulting annual cost savings C_{saved} is the sum of these values subtracted by the sum of OPEX values, see equation 30.

$$C_{var,i} = \frac{C_{Fuel}}{\eta_i}, \forall_{i\,\epsilon\,I} \tag{29}$$

$$C_{saved} = C_{var,el} * E_{ESS,el} + C_{var,th} * (E_{ESS,th} + E_{Tank,th}) - OPEX_{ESS} - OPEX_{PV} \tag{30}$$

Step 11 - Net Present Value Calculation

The final step consists of the economic evaluation of introducing the energy storage technology with the renewable power into the energy system. This is done via a Net Present Value calculation over the assumed thirty year lifetime of the TES.POD. The equation is based on the annual cost savings from avoiding fuel, $C_{saved,n,yr}$, and the multiple CAPEX values, characterized by the index U, see equation 32.

$$U : [Storage, PV, HEX, Tank] \tag{31}$$

$$NPV = \sum_{yr=0}^{30} \frac{-\sum_{u}^{U} CAPEX_{u,yr} + C_{saved,yr}}{(1+r)^{yr}}, \forall_{u \, \epsilon \, U} \tag{32}$$

The results are illustrated as NPV timetables. Figure 18 illustrate an exemplary result of a single NPV calculation for the TES.POD. The figure depict the discounted annual cash flows over thirty years. The cash flows are composed out of the different fuel cost savings and CAPEX values.

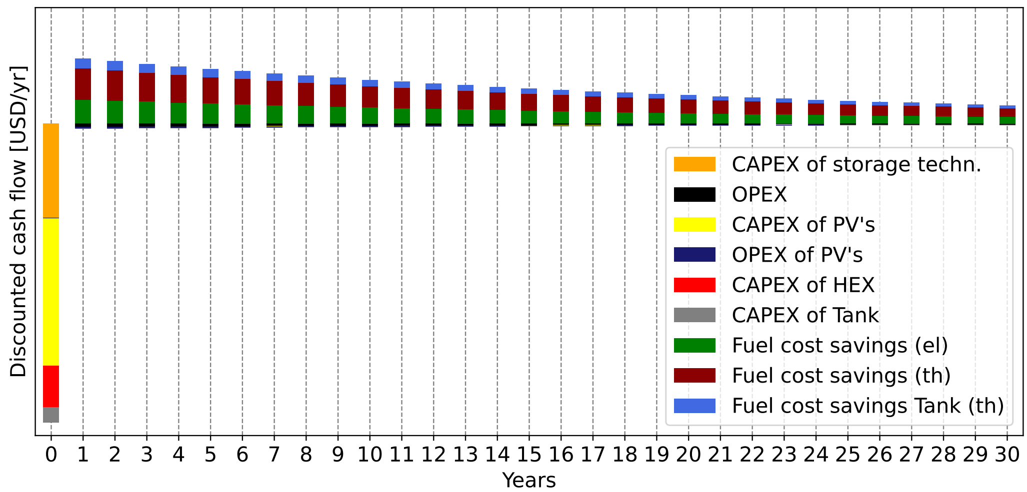

Figure 18: Exemplary cash flow diagram for the TES.POD

Fuel cost savings from discharging electricity is coloured in green, while heat, supplied directly or via a hot water storage tank is presented in dark red and blue, respectively. The negative OPEX value of the storage technology and solar PV's are coloured in black and dark blue, respectively. The CAPEX of the storage system itself is coloured in orange. The CAPEX of the solar PV's is coloured in yellow. CAPEX of the Heat exchanger and water storage tank is coloured in red and grey.

The type of chart visualization was chosen to clearly demonstrate the time dependency and different shares which lead to the result of the NPV calculation. For cost comparisons with other energy storage technologies, different lifetimes could lead to repurchasing requirements which can be illustrated clearly in that type of visualization.

Part III. Results

Literature research across various industries was conducted to identify promising applications. As stated in 4.1, 4 key criteria are required to successfully identify an application as promising and applicable for further analysis. The following list represents the industries that were investigated in this thesis.

- Desalination
- Building Facilities
- Agriculture

Within these industries, different applications and technologies were explored and checked to see if they fulfill all 4 criteria. However, throughout this thesis, it became clear that for most investigated applications, the fundamental analysis was unable to be applied due to a lack of data. The relatively low temperature level of the heat released by the TES.POD excluded many applications which require higher temperatures. Furthermore, specific hourly heat demand profiles for temperatures below 60 °C within an application requiring these temperatures and higher was in many cases hard to find. Publicly available hourly heat demand profiles usually do not distinguish between temperature levels. Construction of hourly heat demand profiles for specific process streams at 60 °C was not possible without detailed process descriptions and schematics for industries requiring heat at a wide range of temperatures, including heat at 60 °C and higher.

The identification of hourly electricity demand profiles as well as process schematics, including water mass flows and temperatures, for specific applications was often unsuccessful. The assumption of generic heat demand profiles was rejected because this thesis aims to produce results based on more accurate data, allowing for a more realistic analysis.

Although the model can be applied to applications with any kind of heat demand, this thesis focused on the heat integration of the TES.POD system. As a result, applications are evaluated if the temperature requirements are met at a temperature of less than 60 °C. It became clear that the required data of heat demand in the range of 60 °C or lower was not detailed enough in applications consisting of process streams requiring temperatures above and below 60 °C. The data of applications with only heat requirements within the temperature range of the TES.POD was easier to access.

The following investigated industries have applications where the heat demand consists of processes only requiring temperatures below 60 °C. Hence, extracting the required data through scientific papers was feasible, making it possible to construct a case with a realistically described energy system.

6. Desalination

Freshwater resources are not equally distributed around the globe and water security is a problem. Potable water is becoming increasingly scarce in certain parts of the globe. Although 70 % of the Earth's surface is covered by water, only 0.5 % of it is potable water available for consumption. 97 % of the available water is salt water. The remaining 2.5 % freshwater resources are to 80 % unavailable, frozen in ice [El-Dessouky and Ettouney, 2002].

Rising water consumption and freshwater pollution coming from increasing population size and increased levels of standard of living is reducing the already small amounts of freshwater resources. High rates of desertification all over the globe is accelerating this process. El-Dessouky and Ettouney [2002] estimates that by 2025, more than 60 % of all world's population will suffer from water shortages. Global availability of potable water is diminishing and by 2030 freshwater availability per capita will decrease by one-third [Cao et al., 2009]. Pakistan for example had in 1951 a freshwater surface availability of 5,260 m^3 per capita, by 2025 this number is estimated to decrease to 700 m^3 per capita [Tahir et al., 2021]. Considering that 70 % of world population lives within 70 km of oceans or seas, desalination plants using seawater to provide freshwater, will increasingly gain in importance [El-Dessouky and Ettouney, 2002].

6.1. Technology types

Desalination processes require saltwater in sufficient quantities. Therefore desalination plants need to be constructed near coastal areas. The produced freshwater must reach areas of consumption which could be located far inland. This requires a potential extensive pipeline system. The removal of salt from seawater requires energy and chemicals. Electricity is mainly used for water pumping while chemicals are used for disinfection processes, chlorine removal, membrane cleaning, mineralization and potabilization. The only residual from the process is called Brine. More than half of it is salt [Aziz and Hanafiah, 2021].

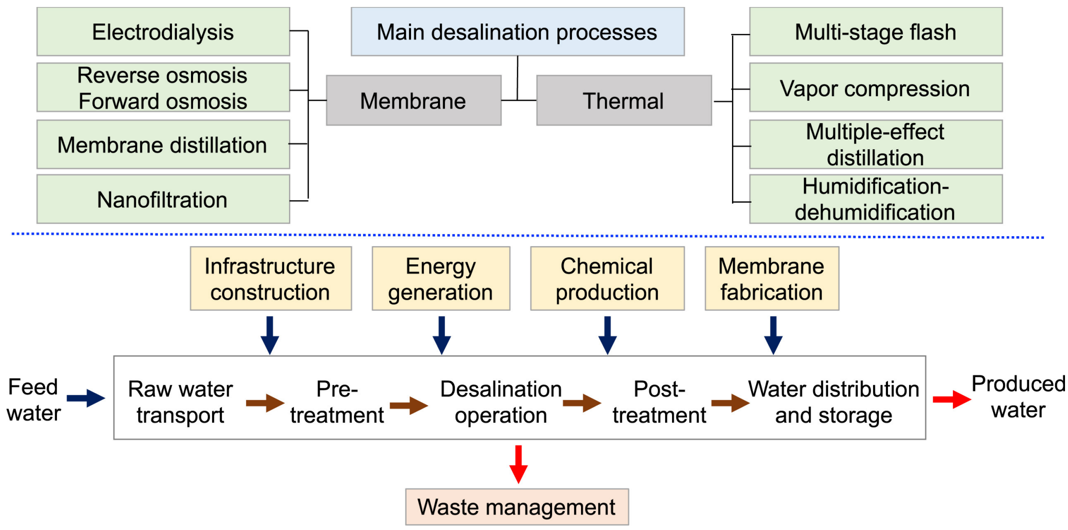

Figure 19: Schematic of existing desalination technologies [Aziz and Hanafiah, 2021]

Figure 19 illustrates all the currently relevant desalination technologies and includes a general process flow chart.

Desalination technology is divided into two main processes, Membrane- and thermal desalination. In between both exist various subgroups. Thermal desalination uses thermal energy to generate vapour in order to separate the salt [Bragg-Sitton, 2015]. Membrane desalination uses electricity to pump the water at high pressures through membranes which separates the water from the salt [Shalaby et al., 2022].

6.2. Market overview

The International Desalination Association state that 18,500 operating desalination plants were in operation in operation in over 150 countries at the end of 2017, with a total capacity of around 99.8 million $\frac{m^3}{day}$ [Lin et al., 2021]. China alone installed 142 desalination plants in 2018 with a production capacity of 1.2 million $\frac{m^3}{day}$ and is planning to increase the capacity to 2.2 by 2020. According to the Global Water Desalination Report published by Visiongain Research Inc., the global market was valued at 14.5 billion USD in 2021 and is estimated to reach 35.5 billion USD by 2035 [VIS].

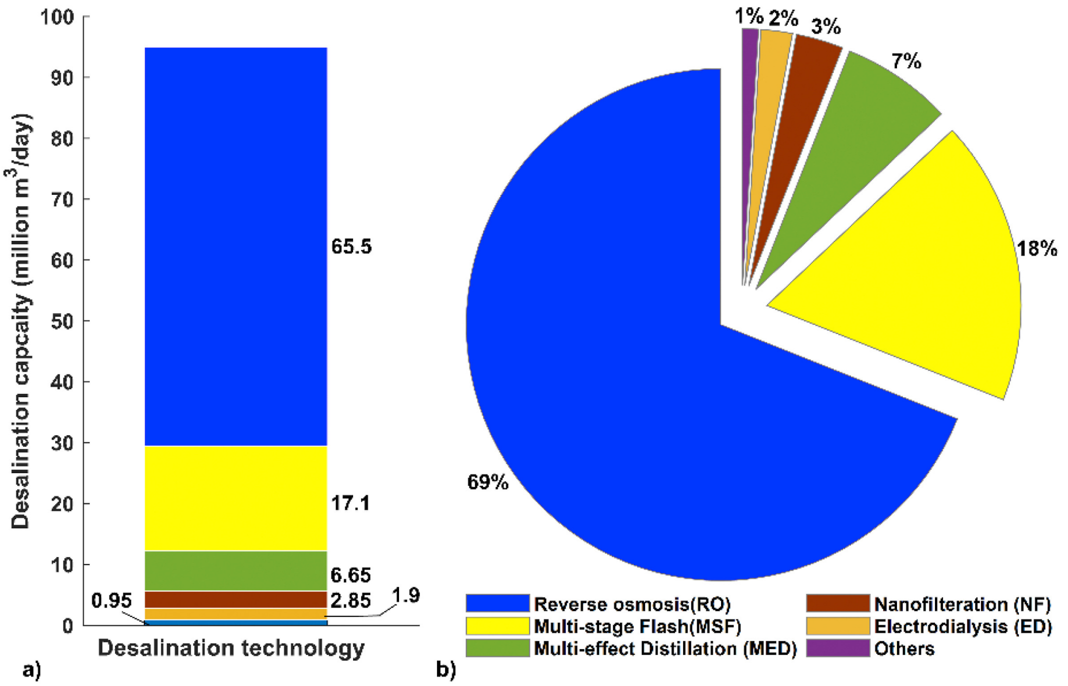

Figure 20: Global installed desalination plant capacity distribution by technology type [Anand et al., 2021]

Figure 20 illustrates the total installed desalination capacity by 2021 in $10^6 \frac{m^3}{day}$ as shares in percent by type of technology. As seen in the pie chart, Reverse Osmosis (RO) dominates the market with 69 %, followed by Multi-Stage Flash (MSF) with 18 % and Multi-Effect Distillation (MED) [Anand et al., 2021].

RO technology is currently the cheapest way to produce freshwater due to no requirement of thermal energy. However, it requires high amounts of electrical energy for high pressure pumping and consumes large amounts of chemicals for membrane cleaning [Shalaby et al., 2022].

MSF and MED are both thermal desalination technologies consuming both high amounts of electrical and thermal energy. MSF was the most dominant technology during the 1980s and 1990s but technological improvements in RO and MED have since then led to decreasing MSF capacities. Although MED has higher initial investment cost, it is considered more cost-efficient due to lower energy requirements which lowers operational cost [MEZ, 2011].

The Gulf states remain an exception following the development of RO. The majority of operating desalination plants are thermal desalination plants. The high salinity of the seawater increases the energy consumption of RO plants and make them less profitable than thermal based technologies [Kim et al., 2020].

6.3. Multi-Effect Distillation

MED desalination has increased in popularity due to attractive characteristics. The process operates at low temperatures and pressures, and is associated with high efficiency as well as low operation and maintenance cost. It is considered economically more feasible, compared to other thermal desalination technologies [Jamshidian et al., 2022]. Although Reverse osmosis quickly overtook the desalination market, thermal desalination is considered better suited for low quality feed water, with high salinity levels [Elsaid et al., 2020].

MED is a thermal vaporizing technology where the natural water cycle through evaporation and condensation is imitated. Unlike RO desalination, this process requires large amounts of thermal energy. Elsaid et al. [2020] states that the specific electricity and thermal consumption to produce 1 m^3 freshwater is 3.5 $\frac{kWh_{el}}{m^3}$ and 6 $\frac{kWh_{th}}{m^3}$ respectively. Compared to other thermal desalination processes, MED can operate at temperatures < 70 °C.

Figure 21 portrays the working principle of a conventional MED desalination plant. The vaporization of saltwater occurs in evaporation chambers called effects. Inside the first chamber, an evaporator provides heat to the incoming salt water stream. Inside the chamber reigns lower pressure levels, thus, vaporization occurs at lower temperatures. This is the reason which allows for low temperature heat sources. The vapour proceeds to flow through a demister to the next effect. The evaporator in effect 2 is heated by the incoming hot vapour from effect 1. The vapour starts condensing inside the evaporator and eventually leaves the system as freshwater distillate. As the vapour condenses and releases heat inside the evaporator, saltwater is fed into effect 2 and is vaporized by the evaporator. This produced vapour is fed into the following effect and the procedure repeats itself in each available effect. Eventually, the vapour from the final effect reaches the chamber containing the condenser. Salt water inside the condenser absorbs the heat from the last vapour stream. The vapour condenses and is removed as freshwater. In each effect, remaining saltwater accumulates on the bottom and is drained as brine [Dastgerdi et al., 2016].

The recovery ratio of MED desalination plants is the reciprocal of the feed to vapour ratio. It describes the thermal efficiency of the process. Typical industry feed to vapour ratios are around 2.857 which corresponds to 35 %.

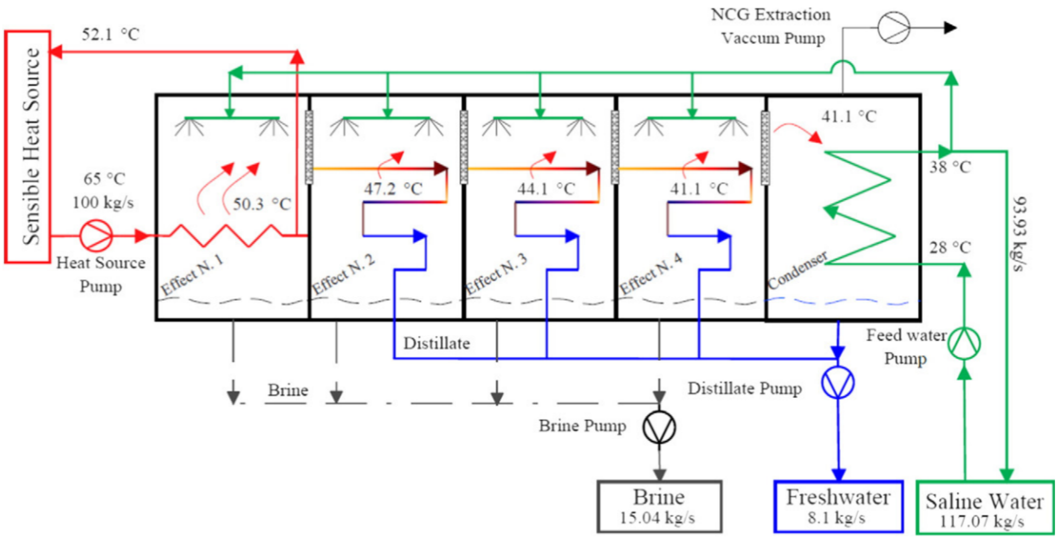

Figure 21: Conventional MED process [Dastgerdi et al., 2016]

The electricity consumption in the system arises from the pumping power requirement across the Heat exchangers and for the vacuum pumps reducing pressure levels inside each effect [Anand et al., 2021].

As in most desalination technologies, energy in most operating MED plants is provided by fossil-fuels. Multiple studies state that waste heat from industries or other power plants could replace fossil fuels due to the low temperature requirements of MED plants. Likewise, solar power as solar thermal collectors with heat engines or hybrid photovoltaic thermal collectors could be used and thus, fulfill the aim of green energy consumption [Anand et al., 2021]. In both cases, electricity and heat demand of the MED plant can be supplied by solar power.

The potential for solar power integration and the low temperature heat requirement makes this type of application interesting for Azelio's TES.POD. The conventional MED schematic 21 shows potential heat feed-in opportunity for the excess heat of the TES.POD in the heat source water stream at the outlet of the first effect at a temperature of 52.1 °C. This process requires one additional heat exchanger, as shown in figure 22.

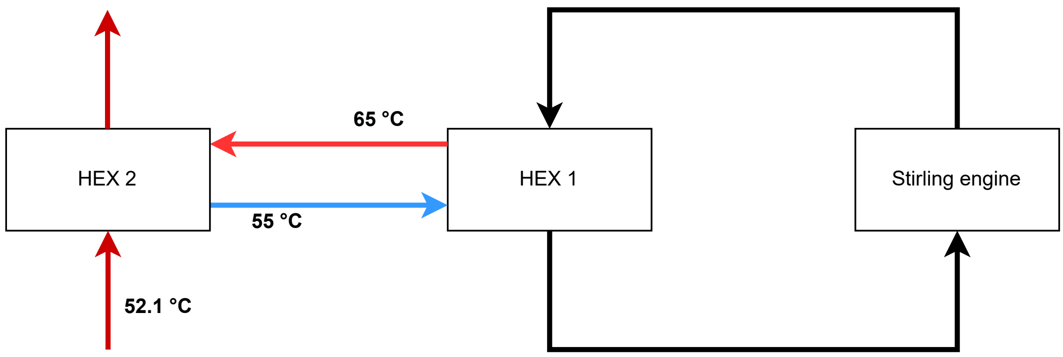

Figure 22: TES.POD integration schematic into the MED plant

6.3.1. Fundamental analysis

The analysis is done by constructing a model of a MED desalination plant, designed to provide a certain amount of freshwater. The freshwater production rate is assumed constant. Hence, the resulting electricity demand profile in figure 23 is constant as well. The figure depicts the demand profile and base-load demand profile at night. The initial freshwater production is 200 $\frac{m^3}{h}$ and the specific electricity consumption (SEC) is 2 $\frac{kWh_{el}}{m^3}$. The SEC value is chosen based on the finding of [Dastgerdi et al., 2016] and [Hesari et al., 2021], where the pumping power requirements for various MED process schemes were calculated and resulted with values between 1.5 - 2.5 $\frac{kWh_{el}}{m^3}$.

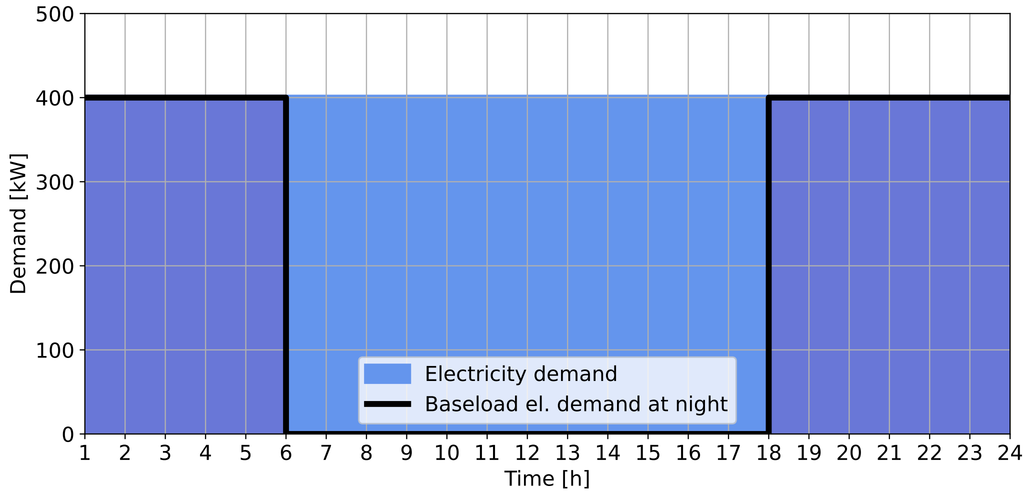

Figure 23: Electricity demand profile of the MED desalination plant with a SEC value of 2 $\frac{kWh_{el}}{m^3}$ and an assumed freshwater production of 200 $\frac{m^3}{h}$.

Because the resulting demand profile is constant at 0.4 MW, base load capacity at night $D_{Baseload,night,el}$ does not differ and is equal to 0.4 MW. At a constant discharge capacity of 10 $\frac{kW_{el}}{TES.POD}$. the amount of units to meet the demand is 40 TES.POD units. The heat generated from these units corresponds to 0.88 MW, assuming 22 $\frac{kW_{th}}{TES.POD}$.

To obtain information about the heat demand for that freshwater mass flow, the various mass flow values in the process schematic in figure 21 were normalized to calculate with the corresponding freshwater production value. The table 6.3.1 shows the calculation procedure for the peak freshwater production of 200 $\frac{m^3}{h}$ (55 kg/s), which result in to a heat-source mass flow of 685 kg/s.

Process streams	Process massflow [kg/s]	Normalized massflow [/]	Model flows [m³/h](kg/s)
Freshwater	8.1	1	200 (55)
Heat source	100	12.35	2,470 (685)
Saline Water	117.07	14.45	2,890 (801)
Saline Water effect 1	(117.07 - 93.93)/4	0.714	142.8 (40)
Brine	15.04	1.86	372 (103)

The corresponding specific heat consumption is calculated with the equation below, and results to a value of 184.5 $\frac{kWh_{th}}{m^3}$. This value is rather high compared to literature values, which range from 6 $\frac{kWh_{th}}{m^3}$, according to Elsaid et al. [2020], and 40 - 60 $\frac{kWh_{th}}{m^3}$ [Al-Karaghouli and Kazmerski, 2013].

$$\frac{\sum_{t=0}^{24} D_{th}(t)}{\sum_{t=0}^{24} m(t)} = \frac{m_{Heatsource} cp(T_{out} - T_{in}) * 24 \frac{h}{day}}{m_{Freshwater}[\frac{m^3}{h}] * 24 \frac{h}{day}} = 184.5 \frac{kWh_{th}}{m^3}$$

In the case of a low literature value of 6 $\frac{kWh_{th}}{m^3}$, the heat demand profile is illustrated in the figure 24. The resulting peak heat demand at 1.2 MW is higher than the heat generated from the TES.POD's, which is why no heat curtailment occurs. At higher values, such as 184.5 $\frac{kWh_{th}}{m^3}$, heat demand increases while the heat generated from the TES.POD units remains the same. Hence, using the calculated value or literature values will not affect the model output.

The MED plant is assumed to be supplied by a natural gas boiler and a natural gas fired combined cycle gas turbine (CCGT). The boiler and CCGT plant efficiency is assumed 80 % and 60 % respectively. The plant is assumed located in the United States.

The fuel cost savings for the Net Present Value calculations of the TES.POD investment were carried out with various natural gas prices, which can be seen in the table 3.

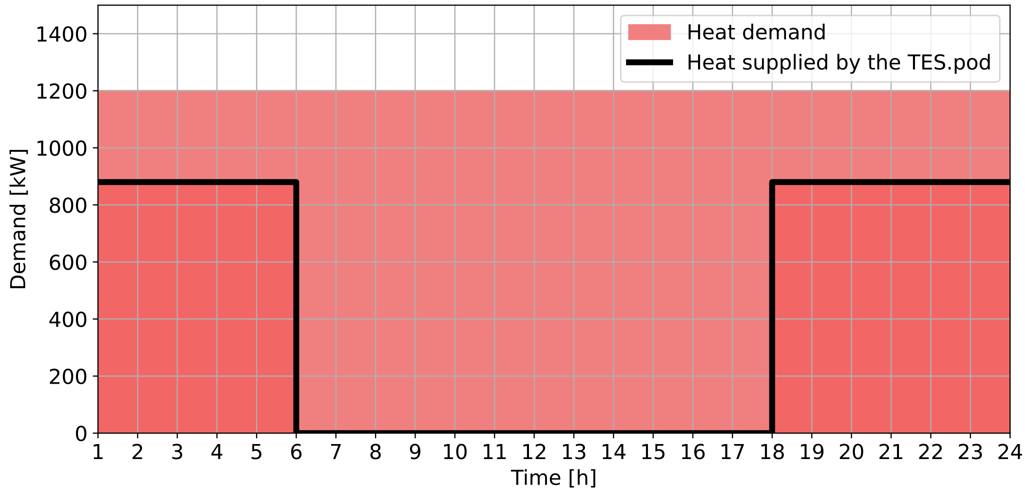

Figure 24: Heat demand profile of MED desalination plant with $SEC_{th} = 6$ kWh/m³ and 200 m³/h freshwater produced

NG price [USD/MMBtu]	NG price [USD/MWh]
4	13.6
6	20.5
8	27.3
10	34.1
12	41
14	47.8
16	54.6

Table 3: Natural Gas Price

Higher fuel prices up to 16 $\frac{USD}{MMBtu}$ are included. According to the natural gas energy outlook U.S. Energy Information Administration, natural gas prices in the United States could rise in the near future to around 16 $\frac{USD}{MMBtu}$, see figure 25.

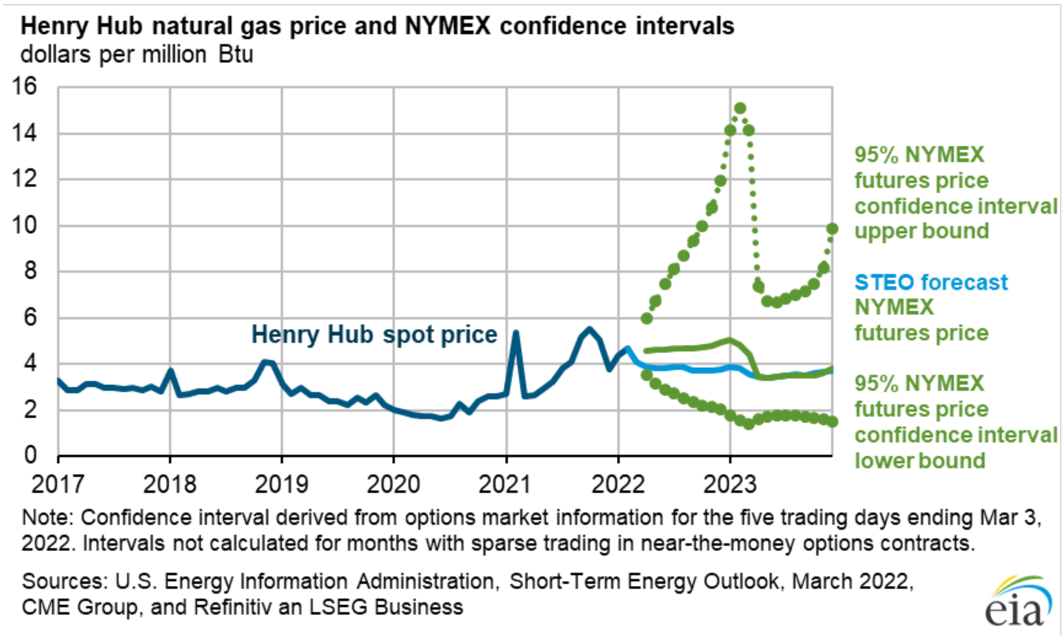

Figure 25: Natural gas price outlook in the United States [U.S. Energy Information Administration].

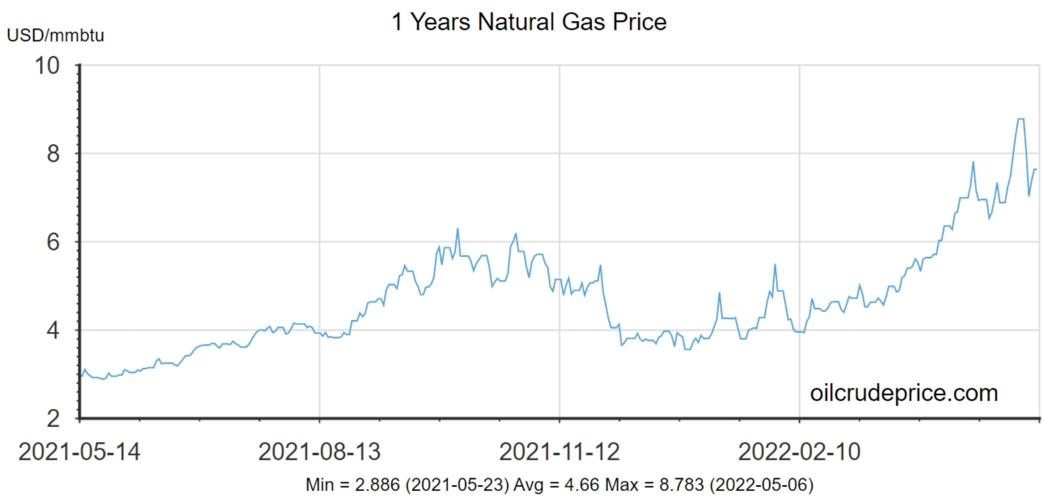

Figure 26: Current natural gas prices in the United States [Oil Crude Price].

6.3.2. Results

In following, an initial default case is created with a chosen fuel price of 8 $\frac{USD}{MMBtu}$/ 27.3 $\frac{USD}{MWh}$ based on the latest found data for the year 2022 in figure 31.

Figure 27 illustrates the results of the analysis which reveals that at that price level the NPV is negative, indicating that the investment of the TES.POD is not desirable from a purely economic perspective, disregarding the CAPEX & OPEX of the existing energy generating technologies and other purchase motivations, such as sustainability and CO2 reductions.

The TES.POD units are able to save 1 752 $\frac{MW_{el}}{yr}$ of electricity which corresponds to 79 707 $\frac{USD}{yr}$. Similarly, 3 854 $\frac{MW_{th}}{yr}$ of directly supplied heat from the TES.POD corresponds to 131 517 $\frac{USD}{yr}$ fuel cost savings. However the OPEX from the TES.POD and the solar PV's reduce the fuel cost savings by 80 %.

Increasing electricity demand does not significantly change the result because without assuming economy of scale, CAPEX and OPEX values proportionally increase with the cash flows. Increasing heat demand at a constantly hold electricity demand, does not change the number of TES.POD units required but also does not increase fuel cost savings, because all the generated heat from the TES.POD's is already completely supplied into the system.

The change in NPV from calculating the HEX CAPEX using Azelio's estimate of 1000 $\frac{USD}{TES.POD}$ instead of using the equation found in the literature has a negligible effect, resulting in a two percent increase.

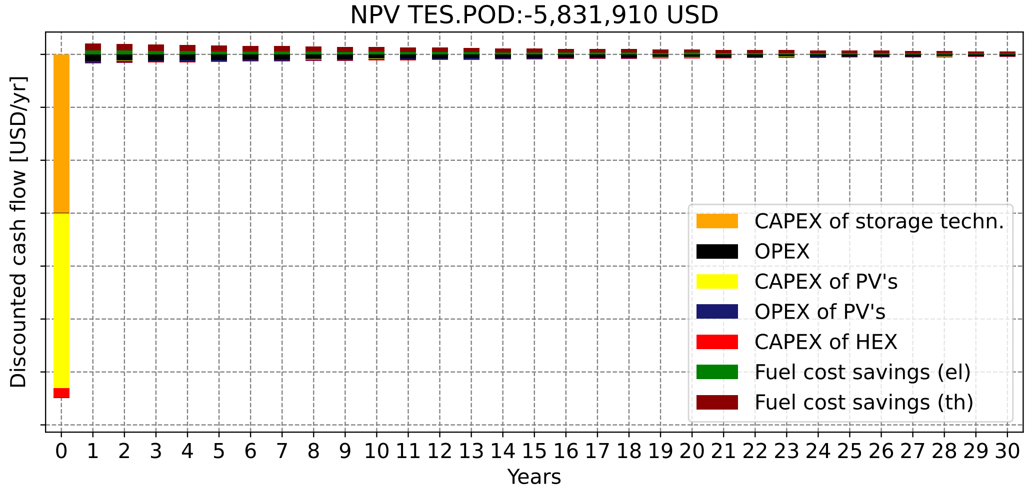

Figure 27: Cash flow diagram for the TES.POD in the MED case study with $SEC_{el} = 2\ \frac{kWh_{th}}{m^3}$ and $SEC_{th} = 6\ \frac{kWh_{th}}{m^3}$ at a natural gas price of 27.3 USD/MWh

6.3.3. Sensitivity Analysis

The sensitivity analysis provides more insight if the TES.POD brings economic value to the system by varying the input parameters. Figure 28 illustrates the NPV results by varying fuel prices and specific electricity consumption values of 1, 2, 3 $\frac{kWh_{el}}{m^3}$, which correspondingly affects the electricity demand profile. As expected, higher natural gas prices lead to increasing yearly fuel cost savings cash flows and lower SEC values results in better NPV's as can be seen by the upwards shifting lines for lower SEC values. The fewer required TES.POD units lower the total CAPEX and OPEX values thus resulting in lower losses. However, the figure shows that across all investigated scenarios the TES.POD is not able to generate positive NPV's by generating enough profits to overcome its CAPEX.

Figure 29 illustrates the findings by varying the capital cost value of the solar PV's. Lower values result in a upward shift of the lines, generating in the case of 450 $\frac{USD}{kW}$ positive NPV's at fuel prices of around 60 $\frac{USD}{MWh}$ and above.

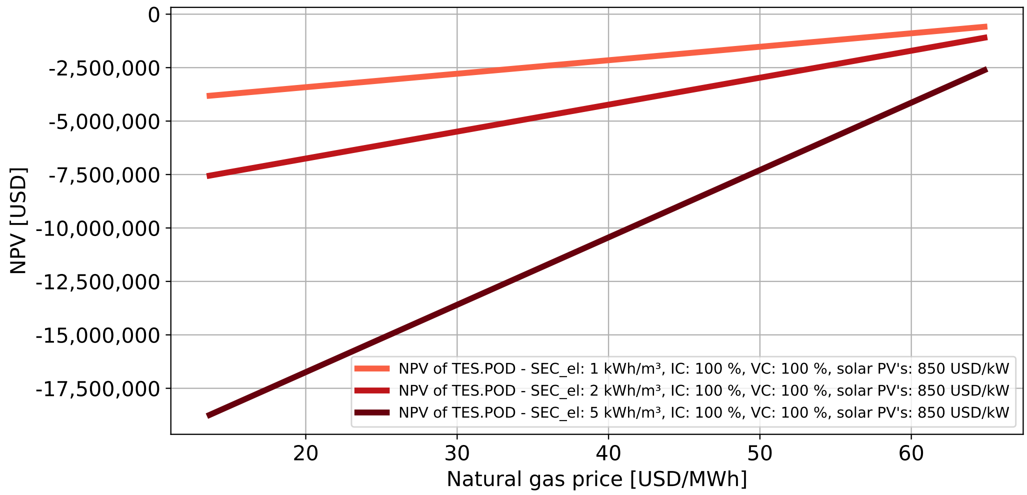

Figure 28: NPV results of the TES.POD in the MED case study for various SEC scenarios between 1,2, and 5 $\frac{USD}{MWh}$, over a range of fuel prices.

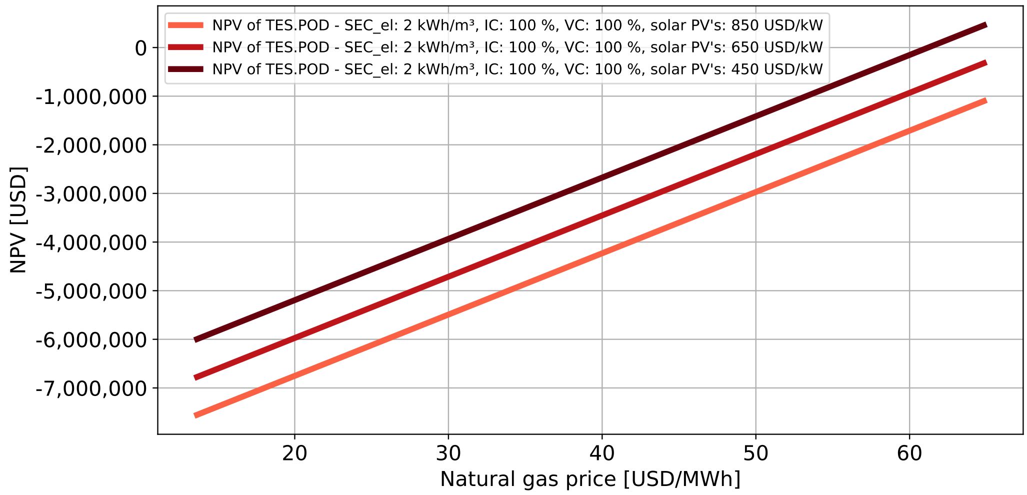

Figure 29: NPV results of the TES.POD in the MED case study for various capital cost values of the solar PV's IC_{PV}, over a range of fuel prices. The SEC value is set at 2 $\frac{kWh_{el}}{m^3}$

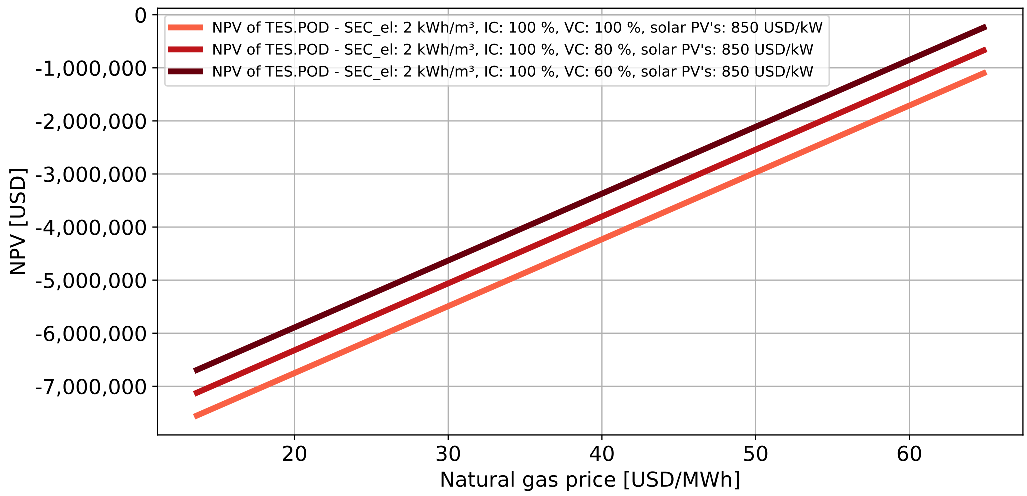

Figure 30: NPV results of the TES.POD in the MED case study for various variable cost VC scenarios, depicted as percentages of the default value, over a range of fuel prices. The SEC value is set at 2 $\frac{kWh_{el}}{m^3}$

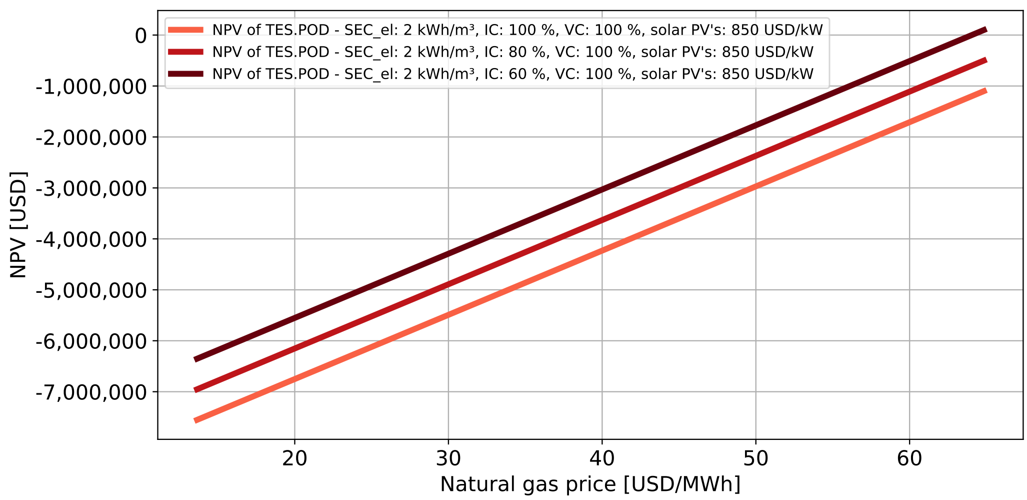

Figure 31: NPV results of the TES.POD in the MED case study for various capital cost IC scenarios, depicted as percentages of the default value, over a range of fuel prices. The SEC value is set at 2 $\frac{kWh_{el}}{m^3}$.

6.3.4. Final remarks

According to the model, data and assumptions for a MED desalination, the TES.POD investment is not profitable. Due to the low cost of natural gas, not high enough value is generated through fuel cost savings to offset the investment cost. However, because of the high heat demand at temperatures below 60 °C, the TES.POD can generate additional fuel cost savings, resulting in better economic performance at certain fuel prices. If a MED desalination facility has other purchase incentives besides profitability, the TES.POD will be a worthwhile addition compared to other ESS if the plant can utilize the heat created.

6.4. Reverse Osmosis

Initially the Reverse osmosis technology was investigated because of its current and increasing high market share in the industry. The standard technology configuration is characterized by only requiring electricity. The feed water is desalinated by forcing it to move through a semi-permeable membrane. This requires high pressure differences across the membrane which are generated with high energy consuming vacuum pumps.

However multiple studies show that higher feed water temperatures reduce pressure requirements due to lower viscosity, higher water diffusivity and increased mass transfer. According to Anand et al. [2021] for each increase in 1 °C, pressure is reduced by 1%.

Figure 32 visualizes the findings. The water flux, shown here in percent, represents the change of fresh water generation for constant feed water flow rate. Both the salt rejection and the water flux are plotted over the feed water temperature. It shows that there is a clear positive correlation for both parameters with increased feed water temperatures. Hence, additional thermal energy supply would benefit the efficiency of Reverse osmosis desalination plants.

Manufactures of reverse osmosis membranes state that the incoming feed water temperature should not exceed 45 °C to not damage the membranes. Those temperatures lie well in line with what Azelio's TES.POD can provide in terms of heat. Assuming feed water temperatures in the range of 2 to 25 °C, heating up to

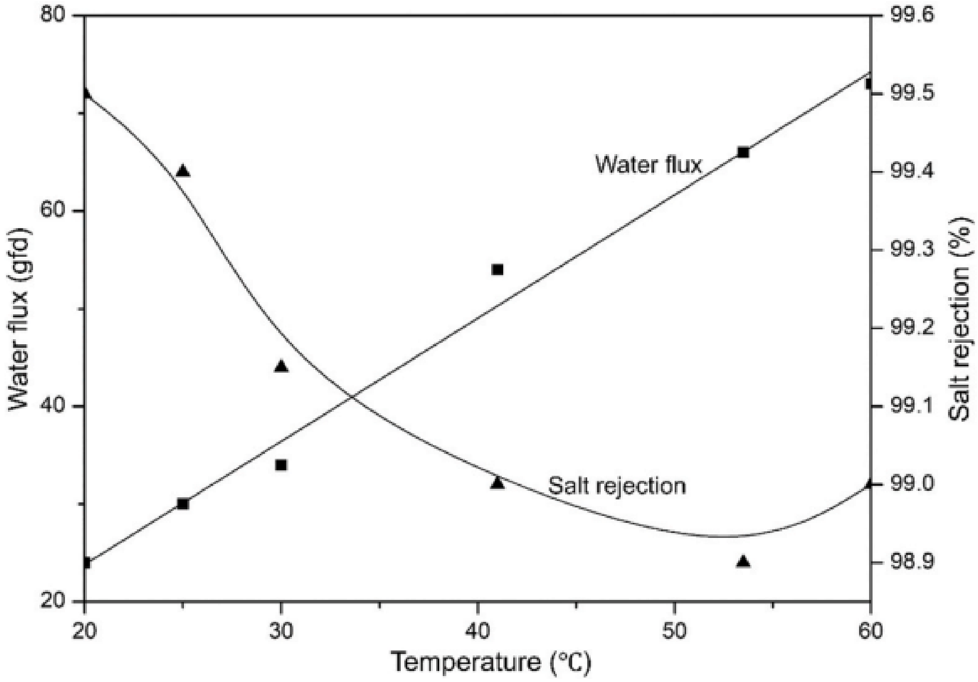

Figure 32: Effect of temperature feed water on water flux and salt rejection is Reverse Osmosis desalination [Anand et al., 2021]

the max. allowed temperature of 45 °C could result to around 20 - 40 % reduced electricity consumption.

But similarly as in the MED case, the electricity demand is designed with a pre-chosen SEC value of for instance 2.5 $\frac{kWh_{el}}{m^3}$. This is hindering because the amount of heat that can be supplied by the TES.POD is directly correlated to the electricity demand. It determines the required amount of power discharge from the TES.POD, which in turn affects the amount of heat generated. Heating up the feed water reduces electricity demand and, so, lowers the electricity discharge output of the TES.POD. Ultimately, this would result in a cycle of decline. By warming up the feed water, the SEC is reduced, which reduces the electric and thermal power output of the TES.POD. Hence, the assumption of a constant specific electric energy consumption value (SEC) would not be accurate and would result in a dynamic real energy system.

No further modelling was constructed because the model can not be applied if the electricity demand is not constant and dependant on the TES.POD output itself.

7. Building Facilities

The building sector is an interesting sector, where Azelio sees potential for the TES.POD as a CHP storage unit. Besides electricity, heat in low temperatures, for instance, space heating, is required. Excess heat from the TES.POD can be directly fed to the building's energy system or into the local district heating system. Considering that around half of the energy consumed in Europe is for district heating purposes and that, globally, investments in district heating systems are increasing, significant business opportunities for Azelio can be identified. As of 2020, 90 % of the global heat consumed was produced by burning fossil fuels. Renewable heat sources, mainly biomass-based, account for only 8 % of total district heat production [IEA, b]. A large variety of other renewable technologies, such as solar thermal and geothermal energy, will increasingly gain in importance. Furthermore, power-to-heat technologies, such as heat pumps, could use excess renewable power to generate the required heat for the district heating system, as it is in the case of Helsinki, Finland [IEA, b].

However, the TES.POD integration into the District Heating system is limited due to supply temperatures. Figure 33 shows the supply and return temperatures of 142 Swedish district heating systems. Supply temperatures vary between around 65 °C and 115 °C [Gadd and Werner, 2014].

Nevertheless, strong incentives exist within the District Heating sector to reduce temperature levels. because a lot of renewable heating options operate at lower temperatures. This implies that buildings, facilities, and piping networks, consuming and distributing the energy must become more energy-efficient. Around 75 % of all existing district heating systems under-perform which results in 12 -20 °C higher temperatures than necessary [TEMPO]. District heating systems operating at supply temperatures over 80 °C experience high heat losses, up to 30 % in the most inefficient systems [IEA, b].

Considering that temperature requirements within building structures and District Heating system will decrease, the potential for the TES.POD will only grow.

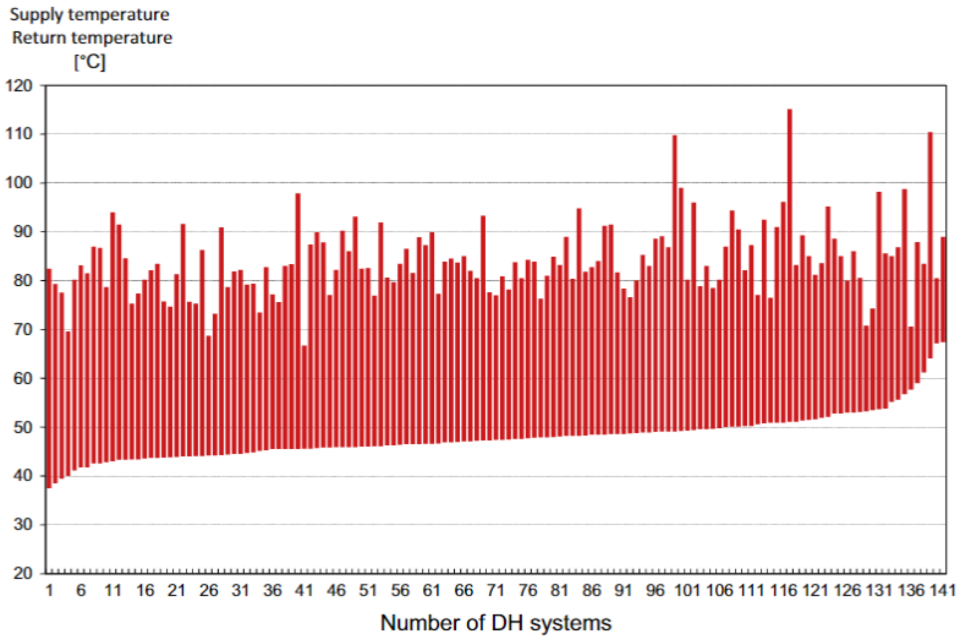

Figure 33: Supply and return temperatures (top and bottom of each bar respectively) in 142 Swedish district heating systems from 2004 to 2010 [Gadd and Werner, 2014]

Within the building sector, hotels and resorts consume a lot of energy. In following, island resorts, are investigated as they are identified as very promising due to location and lack of alternatives.

7.1. Island Resorts

Worldwide, most islands rely on fossil fuels [IRENA, International Renewable Energy Agency, b]. Pacific islands, for instance, rely to 95 % on fossil fuels. Diesel generators primarily deliver the electricity needed for energy related services such as cooking, lightning, water heating, and air conditioning. For instance, the smallest island in Malaysia, Pulau Perhentian relies on diesel generators with a total capacity of 200 kW. Many islands, like in Malaysia, lack electricity resources and therefore need to generate energy locally. The majority of islands are not connected to the national grid [Ashourian et al., 2013].

This makes islands highly exposed to fuel prices, which is a risk factor and can lead to high electricity prices. For instance, in 2012, prices soared to 330 USD/MWh in the Caribbean and Mauritius, and 430 USD/MWh in Hawai. For the same time period, average electricity prices in the EU were 260 USD/MWh. Other factors affecting the price include, long distance to distribution hubs, port size and quality and lack of fuel storage capabilities IRENA, International Renewable Energy Agency [b]. The electricity price volatility influences the cost-competitiveness of inland-located hotels/resorts. Hence, islands have an economic, as well as ecological incentive to increase their share in renewables.

Figure 34 breaks down the share in electricity consumption for different hotel sizes. On average, final energy is consumed mainly for air conditioning, while for very small-sized hotels, hot water production outweighs the air conditioning.

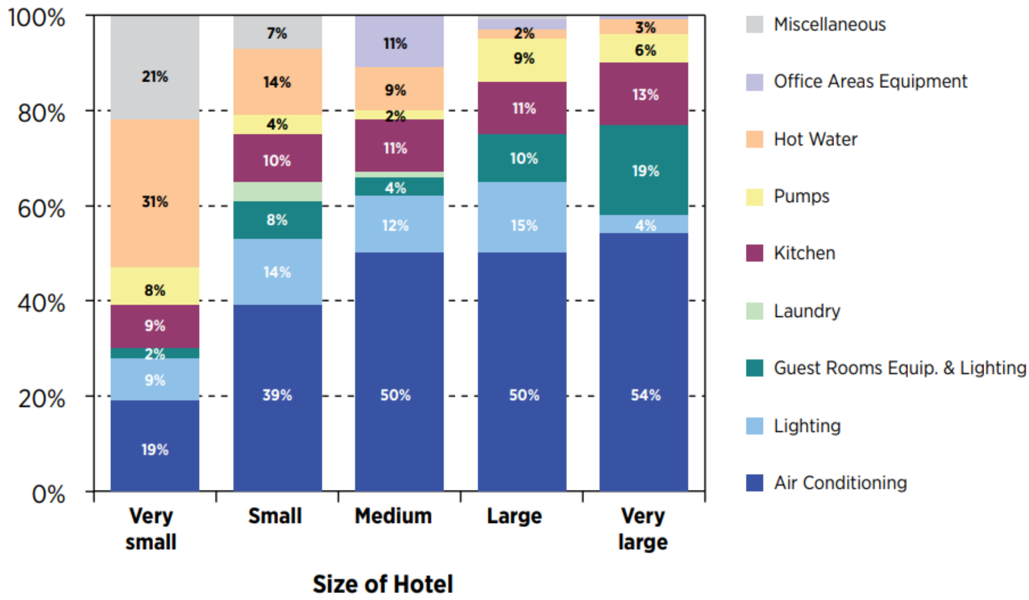

Figure 34: Breakdown of electricity consumption in the hotel sector [IRENA, International Renewable Energy Agency, b]

According to [Weber et al., 2014], heat demand in resorts mainly consist of temperature requirements below < 60 °C. The heat is mainly used for water heating, hot showers and swimming pool temperature regulation.

Especially indoor swimming pools are characterized with continuous high electrical and hot water demand. High water evaporation leads to high humidity levels and reduced water temperatures. If air temperatures drop below dew point, water condensation occurs, which can cause rusting of metals or wood rotting. [Delgado Marín, 2020] states, that relative humidity levels should be maintained lower than 65 %. Hence, the continuous evaporation is counter-fitted by dehumidifying the room, and air temperature levels are maintained generally 2 - 4 °C higher than pool temperatures. These factors impose special energy requirements, which is the reason why indoor pools are associated with high energy consumption levels Weber et al. [2014].

Figure 35 shows the daily heat demand of a 25 m x 12.5 m x 1.8 - 2.2 m indoor swimming pool for a sport facility an Archena, Spain for a typical day in March. The heat is supplied by a biomass boiler during the night, and a solar thermal system during the day. The continuous heat demand of the swimming pool at night indicates potential usage of the excess heat from the TES.POD. Hotels/Resorts with indoor swimming pools have far higher electricity and heat consumption levels. [Cardoso et al., 2018] investigated energy requirements of sport facilities with indoor pools. According to him, indoor pool facilities have energy requirements around 6 times higher than outdoor pool facilities, 666.1 kWH/m^2 and 102.7 kWh/m^2 respectively. Fuel consumption for heat generation during the night can be reduced or replaced by the TES.POD.

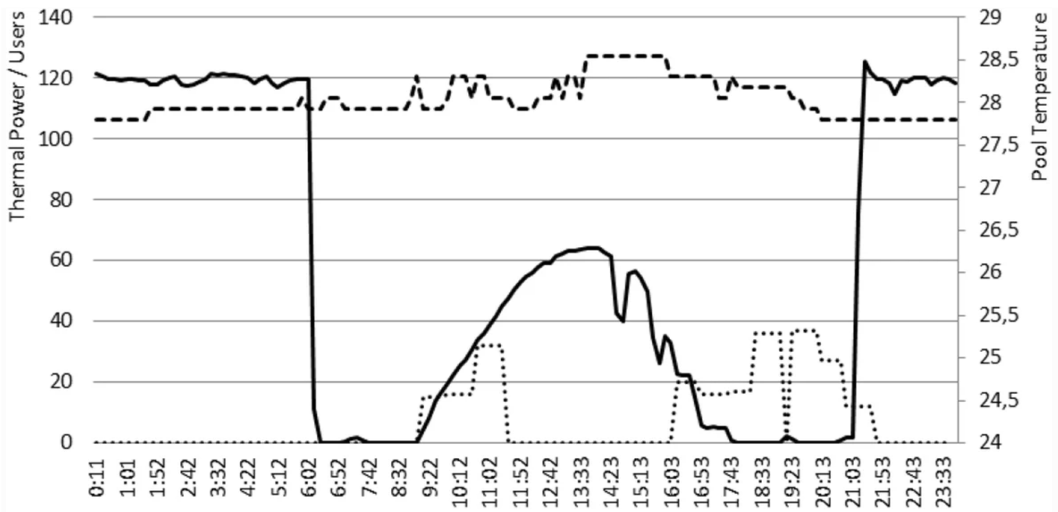

Figure 35: Hourly heat demand in a typical day in March of the Indoor swimming pool in Archena, Spain [Delgado Marín, 2020]

The requirement of demanding electricity and heat in low temperature ranges, makes islands resorts interesting for the TES.POD integration in CHP operation. Additional high energy requiring facilities, such as indoor swimming pools, increases energy demand levels and delivers base-load heat demand conditions, which would increase the profitability of the TES.POD in CHP operation.

7.1.1. Fundamental analysis

The following model is based on the investigation by [Ashourian et al., 2013] of the energy system of the Tioman island, Malaysia which includes a resort and a village. The island records high demand of tourism from February to October, while for the rest, tourism significantly decreases. This notably affects the electricity demand of the island. Hence, two demand profiles, seen in figures 36 and 37, are included in the model for the respective time period.

The bars in light-blue illustrate the electricity demand, while the black line and the dark shaded blue area below shows the base-load demand at night which the TES.POD is able to meet. The demand includes the village and resort located on the island. The main energy applications in the island include, refrigeration, air conditioning, cooking and electricity for lighting and entertainment services.

The peak power consumption in figure 36 is 62 kW, while for figure 37 it is around 8 kW. Peak power demand during that time is at around 8 kW. The total electricity consumption for the high energy demand period sums up to 669 kWh/day. For the low demand period it results to 68.3 kWh/day.

The required battery capacity and number of TES.POD units is determined by the base-load demand of the high demand time period in 36 which is 18 kW. With an assumed constant power output of 10 $\frac{kW}{TES.POD}$, this results in 2 required TES.POD units.

[Ashourian et al., 2013] did not state information about the island's heat consumption or production. Hence, to simulate the heat demand for the island, data about the hot water consumption from typical households in Malaysia in litre per hour was used to generate a normalized heat demand profile [Rahman et al., 2016].

Due to uncertainties about the heat demand profile, various heat demand scenarios were generated with the normalized heat demand profile. According to studies

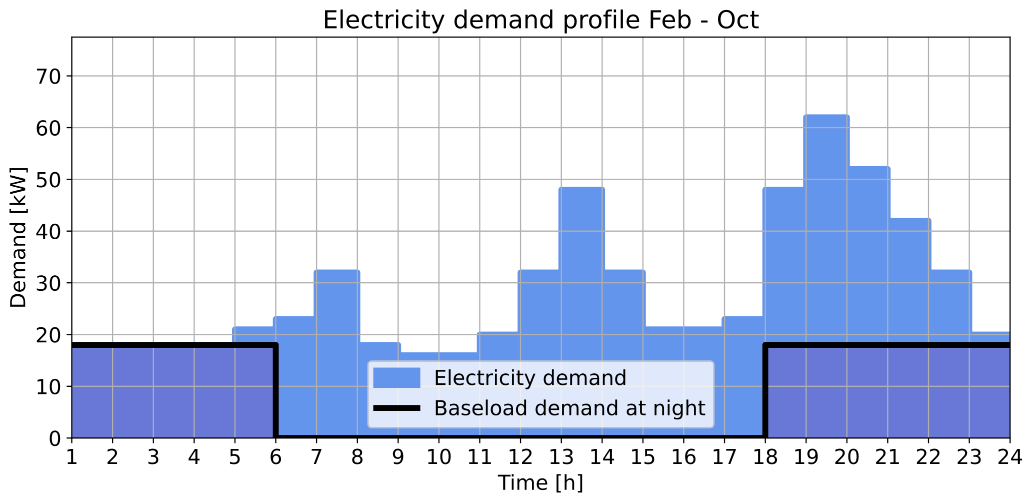

Figure 36: Electricity demand profile with base-load demand at night of the village and resort of the Tioman island, Malaysia for Feb. - Oct. [Ashourian et al., 2013]

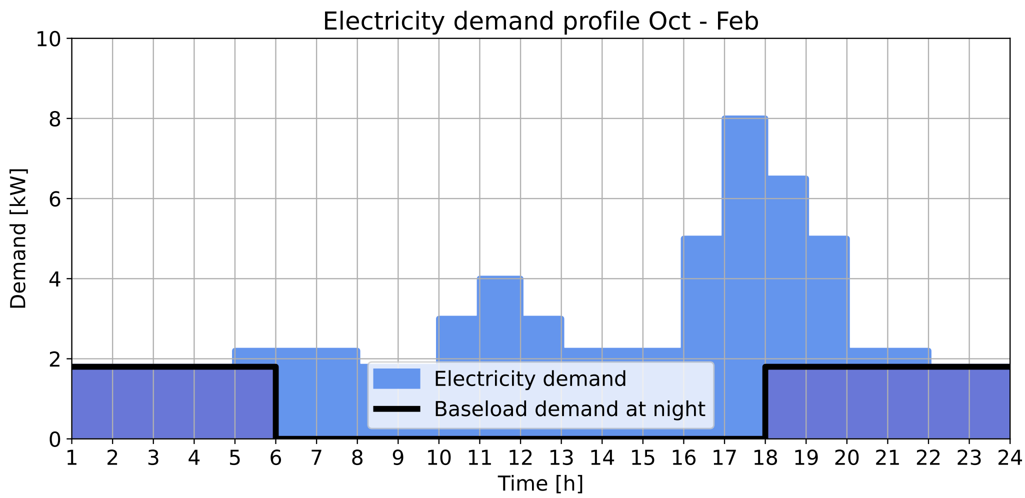

Figure 37: Electricity demand profile with base-load demand at night of the village and resort of the Tioman island, Malaysia for Feb. - Oct. [Ashourian et al., 2013]

from [IRENA, International Renewable Energy Agency, b], around half of the total energy demand in hotels is heat. Considering that the investigated hotel is located in a tropical climate, heat demand values were estimated lower. Hence, the heat demand is represented as a percentage of the electricity demand. The sum of the hourly values of the heat demand corresponds to a fraction of the sum of hourly values of the electricity demand. The chosen heat to electricity demand percentages are 50 %, 25 % and 10%. The following equation illustrates the calculation procedure, using the normalized heat demand profile $D_{th,norm,t}$.

$$T : [0, ..., 24]$$
$$D_{th,t} = D_{th,norm,t} * \frac{\sum D_{el,t} * Percent}{\sum D_{th,norm,t}}, \forall_{t \in T}$$

Figure 38 shows the corresponding heat demand profile, according to [Rahman et al., 2016]. The data is originally available in Litres of hot water per hour. The normalized heat demand profile is calculated with assumed constant return and supply water temperatures. Monthly average ground temperature values in Malaysia at around 27 °C was used for the return temperature and 60 °C for the hot water supply temperature.

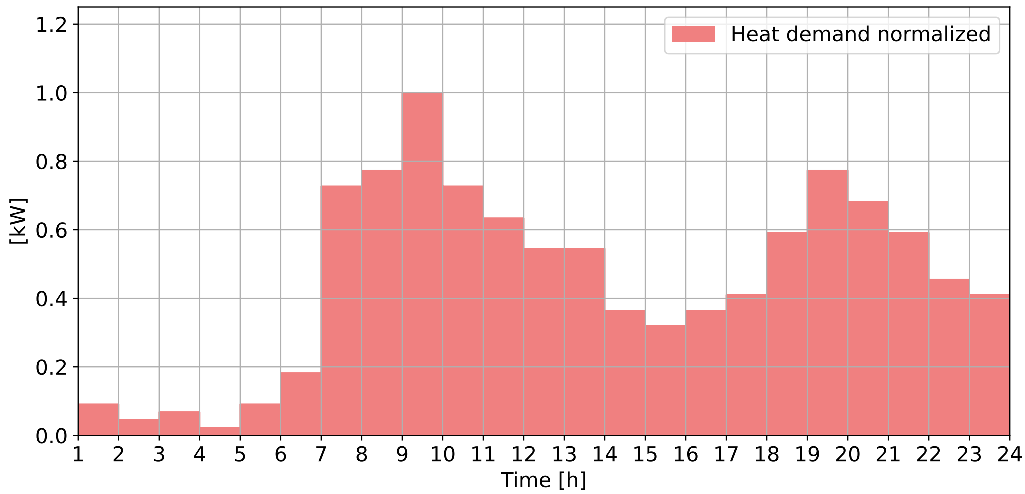

Figure 38: Normalized heat demand profile for an average Malaysian household [Ashourian et al., 2013]

An economic analysis was performed to determine, how much cost savings can be achieved by either the battery or the TES.POD in CHP mode. The Net Present

Value for both technologies was calculated to analyze the cost compatibility between both technologies and the existing energy system. The seasonal differences in energy demand are included. 96 % of the total energy demand is consumed between February and October. 4 % corresponding to 14.5 $\frac{MWh}{yr}$ is consumed in the three remaining months.

The cost savings of introducing the either storage technology were calculated by replacing diesel. The existing energy system of the island consists of a diesel generator, providing electricity and an assumed diesel boiler supplying the heat demanded. The diesel generator- and diesel boiler efficiency were assumed to be 25 % and 90 % respectively. The table below shows the used Diesel price values, which are further used to generate the cost savings of avoiding diesel in the generator and boiler.

Diesel price [USD/L]	Diesel price [USD/MWh]
1	91.2
1.5	136.9
2	182.5
2.5	228.1
3	273.7
3.5	319.3
4	365

Figure 39 shows the corresponding heat demand profile in blue, with a heat to electricity demand ratio of 50 %, for the months February - October. It includes the heat generated from the 2 TES.POD's in light-red and the heat delivered, corresponding to the heat demand in dark-red. Because the TES.POD generates more heat than is demanded, an investment in a hot water storage tank would generate extra fuel cost savings from the otherwise curtailed heat. Therefore, scenarios were created in which the tank is included.

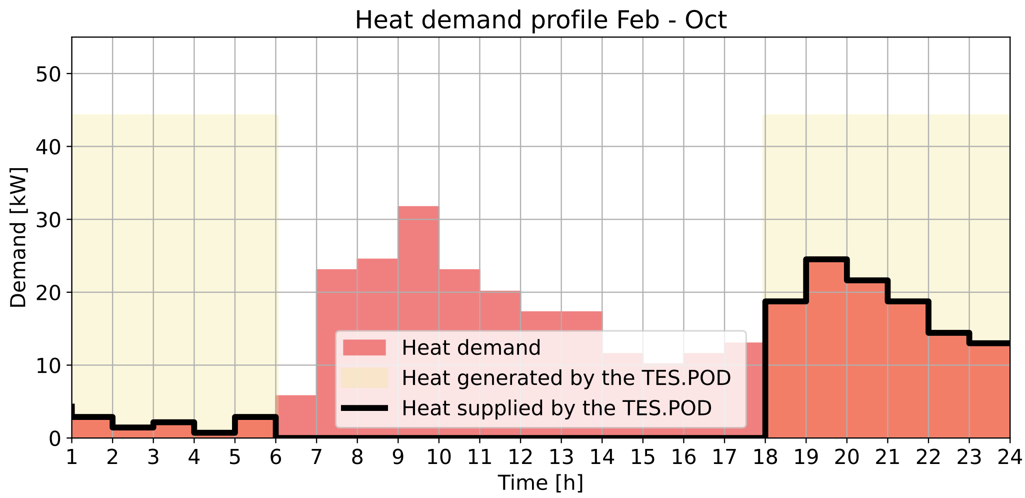

Figure 39: Heat demand profile in blue bars of Malaysian island resort with 50 % heat demand to electricity demand. The light red bars show the heat generated by the TES.POD units in the system and the red bars show the heat demand met by the TES.POD

7.1.2. Results

Figure 40 depicts illustrative results of applying the model for the Island Resort case. The analyzed scenario is carried out with a Diesel price of 3 $\frac{USD}{Litre}$/368.3 $\frac{USD}{MWh}$ and default economic data for the TES.POD. The analysis involves the highest heat demand profile scenario. The heat demand profile is assumed to correspond to 50 % of the electricity demand.

The extra fuel cost savings from an additional hot water tank are included. The tank cash flows are shown in blue. The hot water tank must store 5202 Litre per day which results in a hot water tank CAPEX of 1,561 USD, assuming a capital cots value of 0.3 $\frac{USD}{Litre}$. This value is relatively small compared to the remaining CAPEX components, as can be seen in the figure.

The hot water tank is able to save 56.3 $\frac{MWh}{yr}$ of heat which exceeds that of the heat, directly supplied by the TES.POD of 38.8 $\frac{MWh}{yr}$.

At that fuel price of 368.3 $\frac{USD}{MWh}$ and high assumed heat demand profile, the TES.POD generates enough fuel cost savings to overcome their respective CAPEX. The NPV is positive, indicating that the investment is profitable. However, the heat demand is probably lower in reality.

The change in NPV from calculating the HEX CAPEX using Azelio's estimate of 1000 $\frac{USD}{TES.POD}$ instead of using the equation found in the literature has a negligible effect, resulting in a three percent increase.

Following, a sensitivity analysis is carried out, investigating for instance, assuming lower heat to electricity demand percentages.

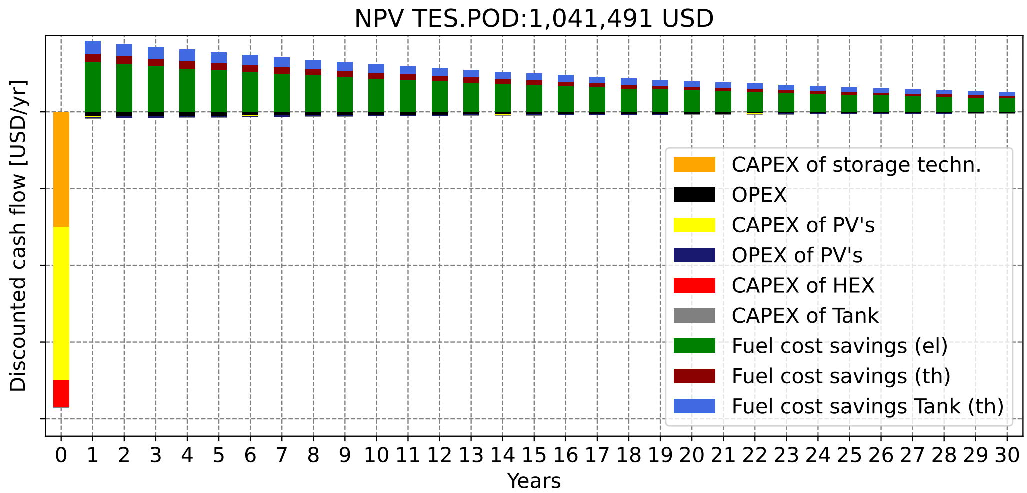

Figure 40: Cash flow diagram for the TES.POD in the Island Resort for an assumed 50 % heat to electricity demand and a diesel price of 91.2 $\frac{USD}{MWh}$. Extra fuel cost savings by including a hot water storage tank are included.

7.1.3. Sensitivity Analysis

A sensitivity analysis is carried out with varying input data. Considering that uncertainties exist regarding fuel prices, technical availability of the hot water tank, heat demand, as well as economic values for the TES.POD, figures, illustrating a more broader range of scenarios were created.

Figure 41 & Figure 42 shows the results of the NPV calculation for various heat to electricity demand ratio scenarios across a broad range of fuel prices. Figure 41 analyses the scenarios with the integration of hot water storage tank and figure 42 without it. Both figures show that the NPV becomes negative at very low fuel prices around 100 $\frac{USD}{MWh}$ or lower. Similarly, higher heat demands results in an upward shift of the line, increasing the profitability of the investment. In comparison, the heat tank inclusion increases the profitability of the investment significantly.

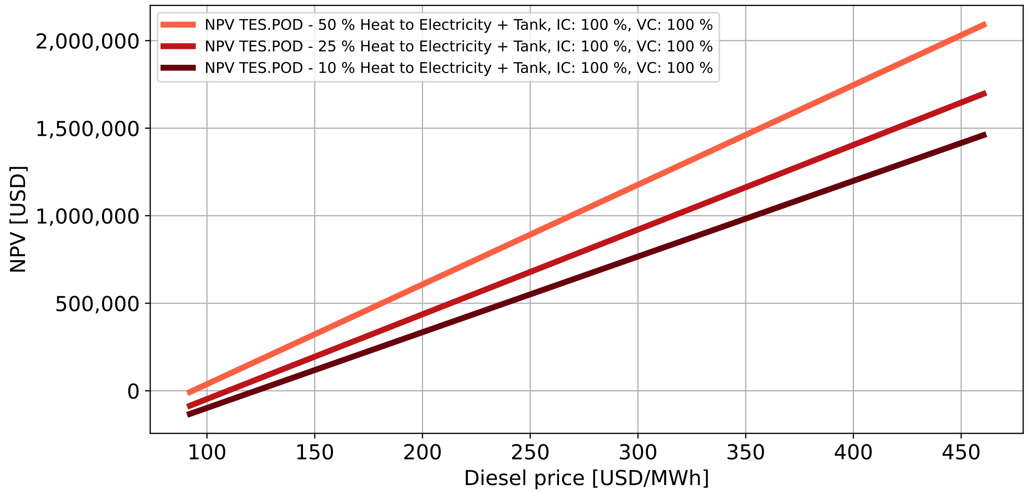

Figure 41: NPV results of the TES.POD in the Island Resort case, including a hot water storage tank, for various heat-to-electricity demand scenarios over a range of fuel prices.

Figures 43 and 44 similarly depict the NPV results as in 41 but instead of varying heat to electricity ratios, the ratio is set at 10 % and the effect of varying economical parameters of the TES.POD is investigated. Figure 43 investigates varying the variable cost and figure 44 investigates varying TES.POD capital cost IC, both represented as percentages of the default value.

Both figures show that either lowering the variable cost or investment cost results in an upward line shift, increasing the profitability of the investment but the affect is small and does not significantly increase the investment.

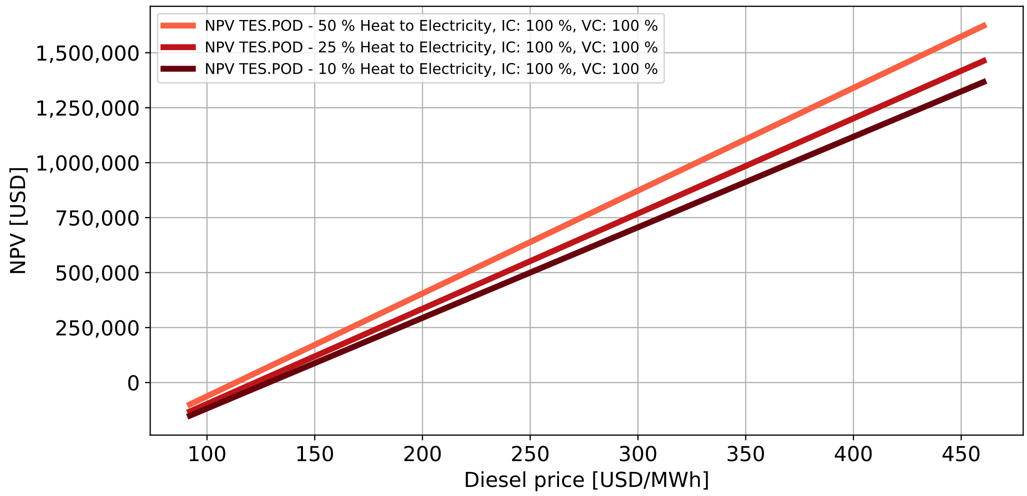

Figure 42: NPV results of the TES.POD in the Island Resort case, without a hot water storage tank, for various heat-to-electricity demand scenarios over a range of fuel prices.

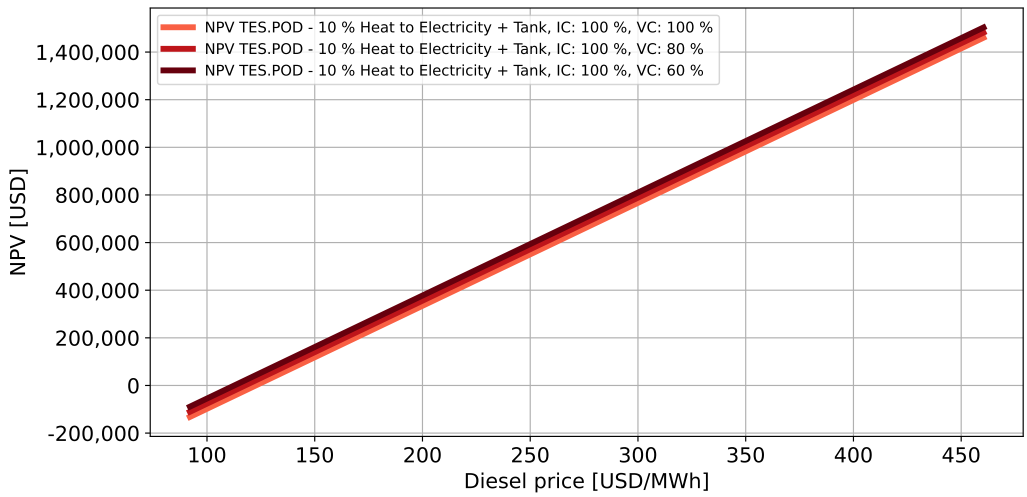

Figure 43: NPV results of the TES.POD in the Island Resort case, including a hot water storage tank, for various variable cost VC scenarios and a 10 % heat to electricity demand over a range of fuel prices.

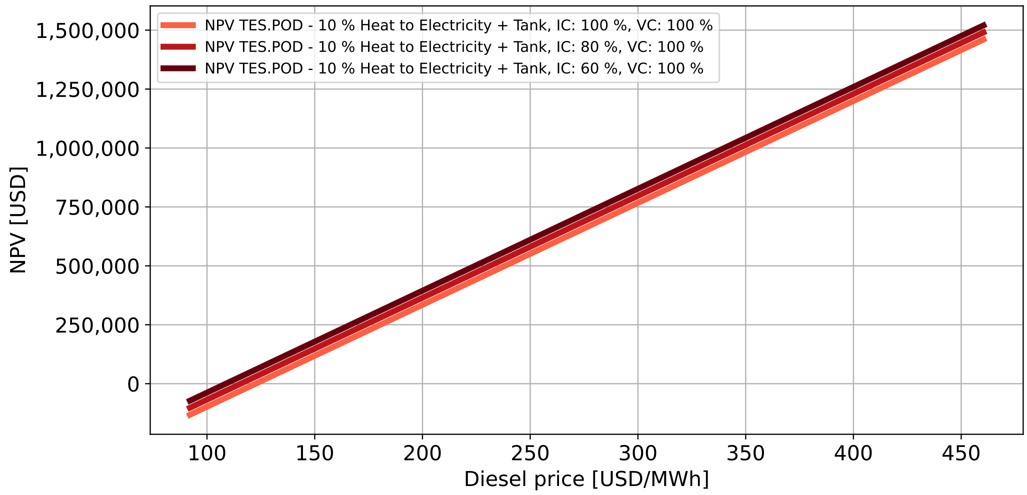

Figure 44: NPV results of the TES.POD in the Island Resort case, including a hot water storage tank, for various capital cost IC scenarios and a 10 % heat to electricity demand over a range of fuel prices.

7.1.4. Final remarks

To conclude, island resorts have strong incentives to increase their share in renewables. The dependence on fossil fuels to generate energy is affecting the market competitiveness with other market players, located more in-land. The fluctuating and increasing fuel prices is a future risk factor. The geographic location of island resorts, mostly located in tropical climates, such as South-East Asia and the Caribbean, allows for high shares of solar power integration. The heat demand in warmer climates is comparably lower than in colder regions. This means that heating mostly is used for water heating, such as, for showers or pool heating. The economic investigation based on the Tioman island indicates that the TES.POD in CHP operation can, depending on the heat demand and fuel price, bring economic value to the system. The introduction of a hot water storage tank significantly increases the cost compatibility. However, assuming high values of heat demand, such as 50 % heat to electricity demand, is uncertain considering that the island is located in a tropical climate in Southeast Asia. The amount of heat to electricity demand ratio could be lower than 10 %, although the existence of indoor swimming pools would notably increase the heat demand. Furthermore, the inclusion of storage tanks are uncertain too because the island could possibly meet their hot water demand during the day with other solar-based technologies.

But overall, the NPV calculations indicate that the TES.POD investment is interesting and should be further investigated. Islands with fairly high heat demands where a hot water tank inclusion is possible, the TES.POD investment becomes very profitable, considering that fuel prices are uncertain and expected to increase further. The investment makes sense even if diesel prices go below 100 $\frac{USD}{MWh}$ and NPV's go negative.

8. Agriculture

Agriculture is the world's largest industry sector. Since the industrial revolution, the industry has shifted from intensive manual labor to heavy machinery. That shift is accompanied by increased fossil fuel consumption to provide the necessary energy.

Because of the need for reliable long-duration renewable energy as well as current low temperature requirements, Azelio has identified the agriculture industry, including food processing and beverage plants, as promising. Azelio has identified the agriculture industry, including food processing and beverage plants, as promising because of the need for reliable long-duration renewable energy as well as present low temperature requirements.

In the following, a greenhouse case study is investigated using company internal data of a potential customer.

Throughout this thesis, dairy plants and breweries have been investigated because of their large economic share in the industry and process requirements of 100 °C or lower. Although literature research concluded that the TES.POD has potential for integration in CHP mode, no further investigation was carried out due to a lack of data, such as process schemes and energy demand profiles.

8.1. Greenhouses

Greenhouses are building structures in which agricultural products can grow under optimal climate conditions, decoupled from outside conditions. Colder countries, such as the Netherlands and Belgium, operate large numbers of greenhouses to obtain agricultural products year round. However, sustaining optimal growing conditions inside the greenhouses requires energy.

Energy is more often provided by burning fossil fuels, which is why there is a growing incentive in the greenhouse industry to implement more sustainable energy generation measurements [van Beveren et al., 2019].

Figure 45 illustrates a general schematic of the energy system of conventional greenhouses [Van Beveren et al., 2015]. The figure shows that a number of factors affect indoor conditions, such as temperature and humidity level. Factors affecting the indoor temperature T_{air} are solar radiation Q_{sun}, convective heat losses Q_{conv}, crop transpiration losses Q_{trans}, heat from artificial lighting Q_{lamp}, heat losses due to ventilation Q_{vent}, heat added from water pipes Q_{pipe} and heating and cooling from heat exchangers $Q_{he,heat}/Q_{he,cool}$.

Humidity levels X_{air} is influenced by crop transpiration ϕ_{trans}, condensation ϕ_{cov}, cooling $\phi_{he,cool}$ and ventilation ϕ_{vent}.

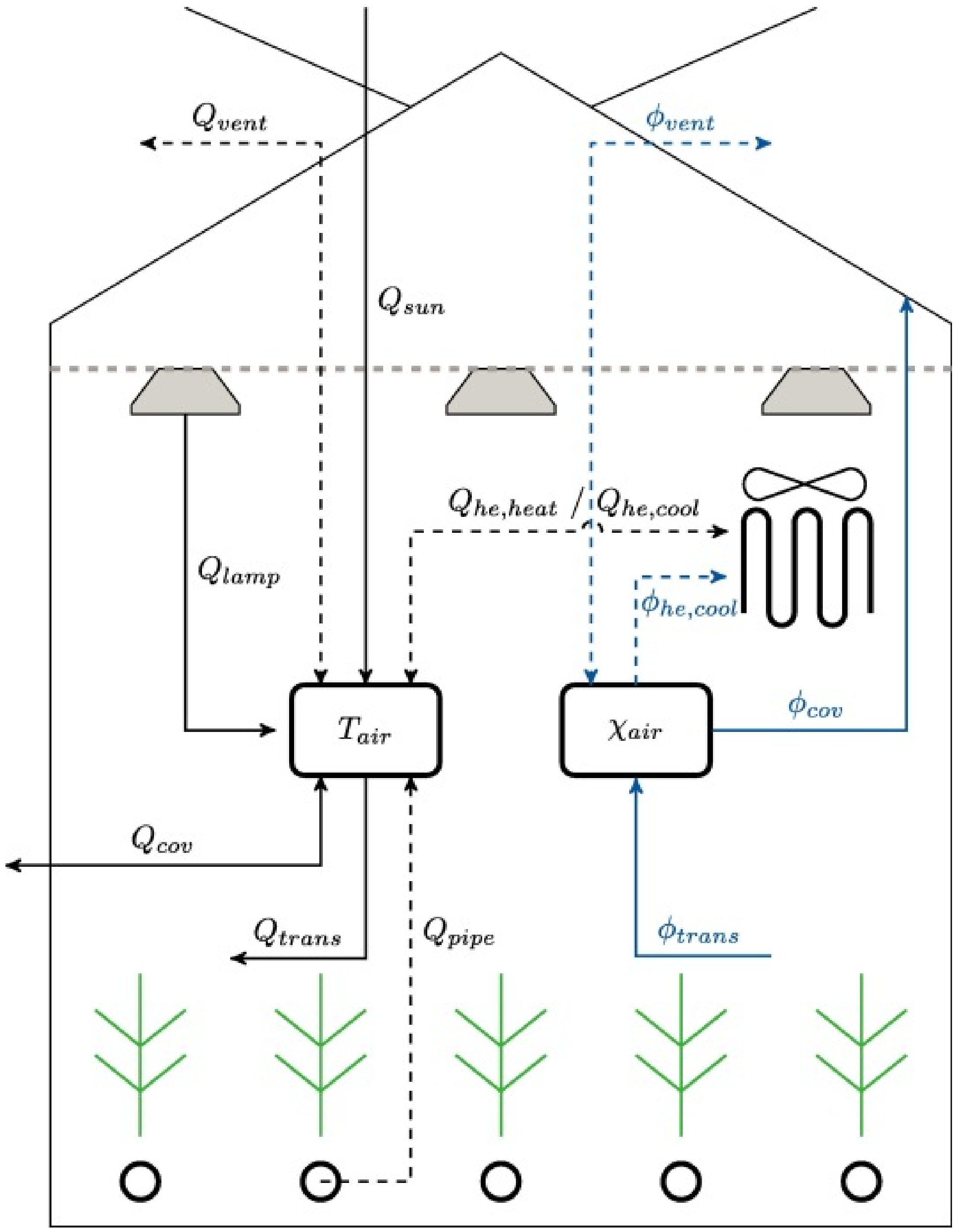

Figure 45: Greenhouse energy system schematic [Van Beveren et al., 2015]

Electricity is required for the lamps, pumps, and ventilation system. If harsh outside conditions demand external heating or cooling, a hot water piping system, heat exchangers, and/or electrical heaters will regulate inside air temperatures.

While electricity demand occurs more steadily, heat demand fluctuates more dependently on outside conditions. As figure 45 indicates, modelling the energy demand in greenhouses requires complex, dynamic climate modelling.

While electricity is steadily consumed for artificial lighting, pumping and ventilation, heating and cooling requirements are influenced by outdoor temperatures, humidity, CO2 concentrations, and lighting conditions. Furthermore, different climate conditions apply depending on the type of plants being cultivated and the respective growing conditions [Van Beveren et al., 2015].

If greenhouses are heated via a hot water pipe system, the pipes are located close to the growing plants. The air around the crops is heated. Water temperature requirements are low at around 60 °C [Bartzanas et al., 2005]. Steady electricity demand and the low temperature requirements make greenhouses an interesting case for the TES.POD integration as a CHP unit.

8.1.1. Model description

In the following, a potential application is investigated based on company internal data of a potential customer in the agriculture industry in Arizona, USA. The customer's energy systems rely on uncertain grid electricity and natural gas for heating for their respective greenhouse complexes. Hence, the incentive for the TES.POD investment exists to generate more sustainable energy and to obtain back-up power. Furthermore, Arizona has good conditions for solar power integration.

Figure 46 depicts the provided data of the application's electricity demand for one year. The demand profile is valid for the time period between July 2020 and July 2021. At the start of the year 2021, a clear increase in demand is depicted, with peak power levels of over 800 kW. The calculated base-load demand during the night is included as a dark blue shaded area under a black line at 50.8 kW.

That value results in 6 TES.POD units being required. However, within figure 46, it can be seen that for the majority of the year, a better predicted estimate of the base load demand is around 200 kW. This corresponds to 20 TES.POD units.

Figure 47 depicts a mean average 24 hour electricity demand profile with a base load demand at night of 266 kW, corresponding to 27 TES.POD units.

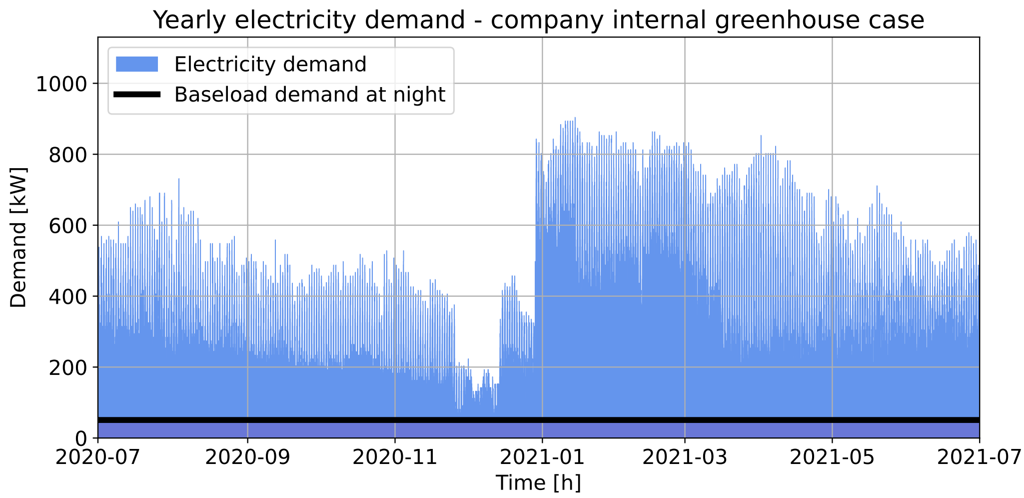

Figure 46: Electricity demand profile over one year of the greenhouse case study with company internal data.

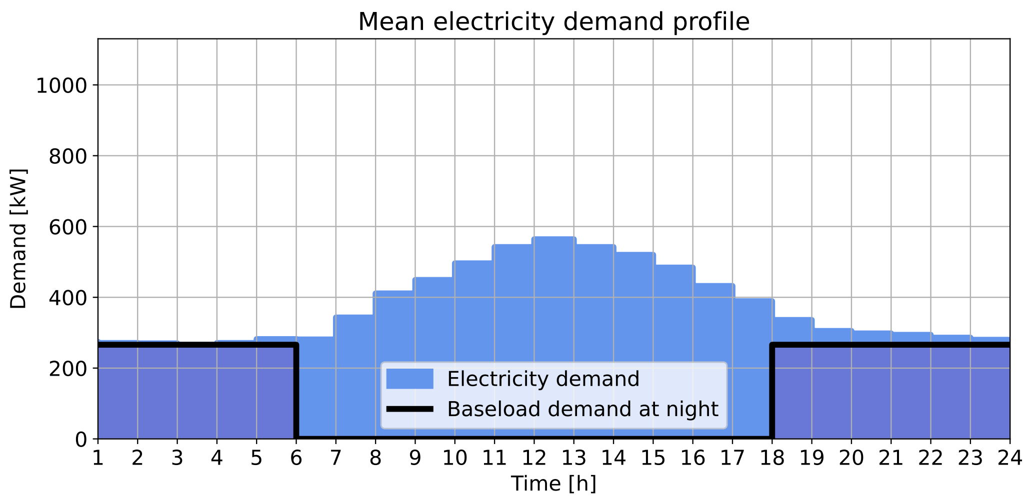

Figure 47: Hourly mean electricity demand profile for one day of the greenhouse case study calculated with company internal data depicted in figure 46

Data about the customers' heat demand profile and exact information about the existing energy generating technologies are not provided, thus in order to apply the model, missing data must be estimated through literature research. Due to a lack of data and time limitations, conducting a climate model to estimate the heat demand of the customer was not possible within the framework of this project.

[van Beveren et al., 2019] investigated the energy system of a 40,709 m^2 greenhouse area in the Netherlands with measured data for electricity and heat demand profiles. The energy demand is met via a natural gas boiler, a CHP plant, and the power grid.

The data is not publicly available, but a few selected demand profiles are provided. It can be concluded that greenhouses are characterized by a regular pattern of electricity demand compared to heat demand.

Similarly, [Ozturk and Kucukerdem, 2016] investigated the heat demand in greenhouses located in Andana, Turkey. The results are presented as monthly values. Although various scenarios were investigated, the results clearly depict an outside temperature dependency, resulting in higher heat demand during the winter months and falling to zero for the majority of the summer months. Despite the fact that many factors affect the heat demand in greenhouses, outside temperatures mainly influence the amount of required heat. Considering that the client's location in Arizona, USA, deals with similar temperature levels as in Adana, Turkey, a similar trend throughout the months can be assumed. The monthly temperature values for Phoenix, Arizona, as in high and low values, are found in table 4.

In the winter months, temperatures fall below 10 degrees, indicating that heating requirements at night are probably needed.

Considering the fact that the heat demand can be classified in the same value range as electricity [van Beveren et al., 2019], scenarios were created with heat to electricity demand percentages of either 100 %, 50 % or 20 % . Based on the findings of [Ozturk and Kucukerdem, 2016], assuming a constant heat demand profile throughout the whole year does not depict the yearly heat demand in greenhouses accurately. Hence, similarly to the findings of [Ozturk and Kucukerdem, 2016] a normalized monthly heat demand profile was created in figure 48.

Furthermore, a general normalized heat demand profile for 24 hours was created, see figure 49.

The peak heat demand value is calculated in equation 36 which is dependant on the time dependant percentages in figures 48 and 49 $D_{th,norm,t}$ and $D_{th,norm,m}$, as well as on an average peak electricity value $P_{el,mean}$ based on the electricity demand

Months	Temperature Max [°C]	Temperature Low [°C]
January	20	8
February	22	9
March	27	13
April	31	17
May	34	20
June	41	27
July	41	29
August	41	29
September	38	26
October	32	19
November	25	12
December	20	8

Table 4: Phoenix, Arizona monthly temperature values in [°C] Current Results

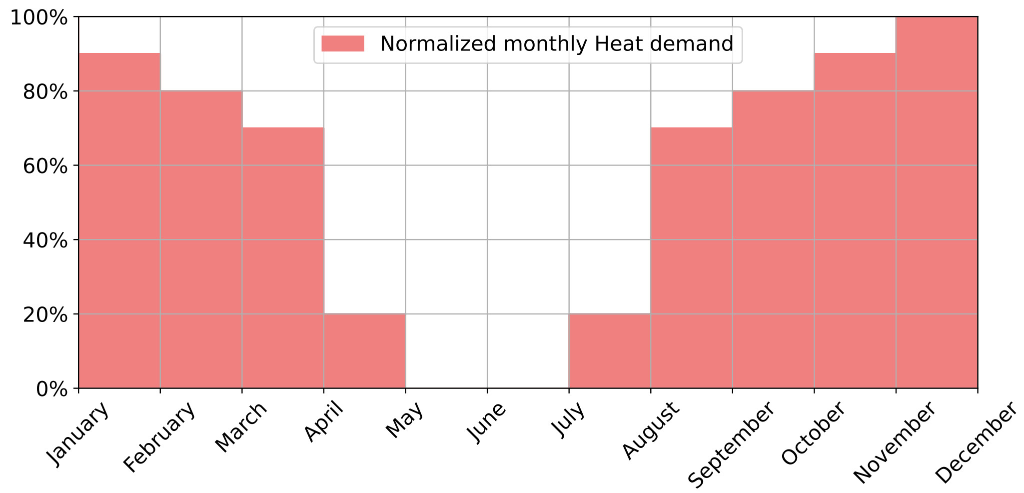

Figure 48: Normalized monthly heat demand profile $D_{th,norm,m}$ for the greenhouse case study.

in 47, see equation 33. The result is multiplied by the assumed heat-to-electricity demand percentage, $\frac{Heat}{Electricity}$ which can be either 100, 50, or 20 percent.

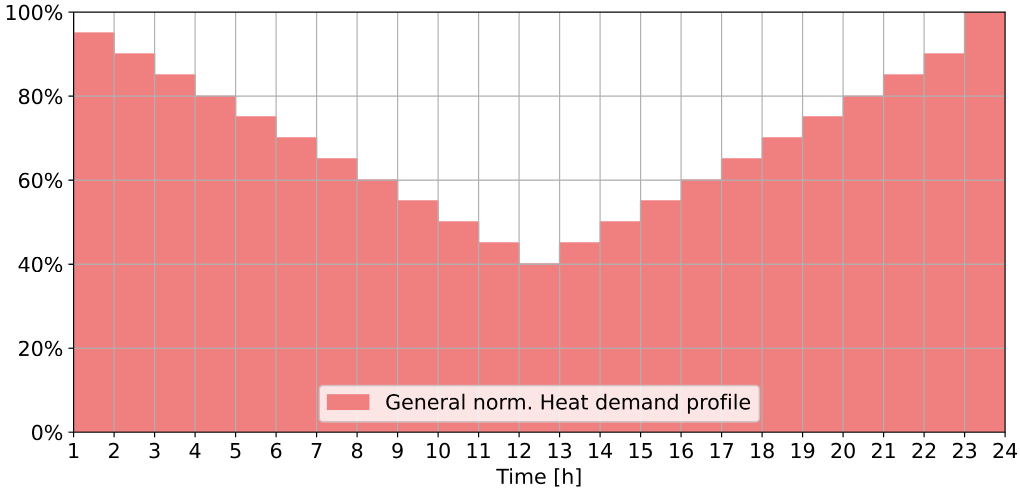

Figure 49: General normalized hourly heat demand profile $D_{th,norm}$ for one day for the greenhouse case study.

$$P_{el,mean} = \frac{\sum_{t=0}^{24} D_{el}}{24} \tag{33}$$

$$M : [January, ..., December] \tag{34}$$

$$Percent : [100\%, 50\%, 20\%] \tag{35}$$

$$D_{th,t} = D_{th,norm,t} * D_{th,norm,m} * P_{el,mean} * \frac{Heat}{Electricity}, \forall_{m,t \, \epsilon \, M,T} \tag{36}$$

Figures 50 and 51 illustrate the resulting heat demand profiles for January and August, using a 100 % heat to electricity demand percentage and a $P_{el,mean}$ of 370.5 kW, respectively.

Both figures indicate that the heat generated by the TES.POD units exceeds the demand at all times. Hence, including a hot water tank will generate extra fuel cost savings by supplying the heat demand during the day. Figure 52 illustrates the heat demand profile for December, which includes a hot water storage tank. As can be seen, the otherwise curtailed heat exceeds the demand during the day and, thus, is able to supply the demand during the day. In the following, the inclusion of a hot water storage tank is always presumed.

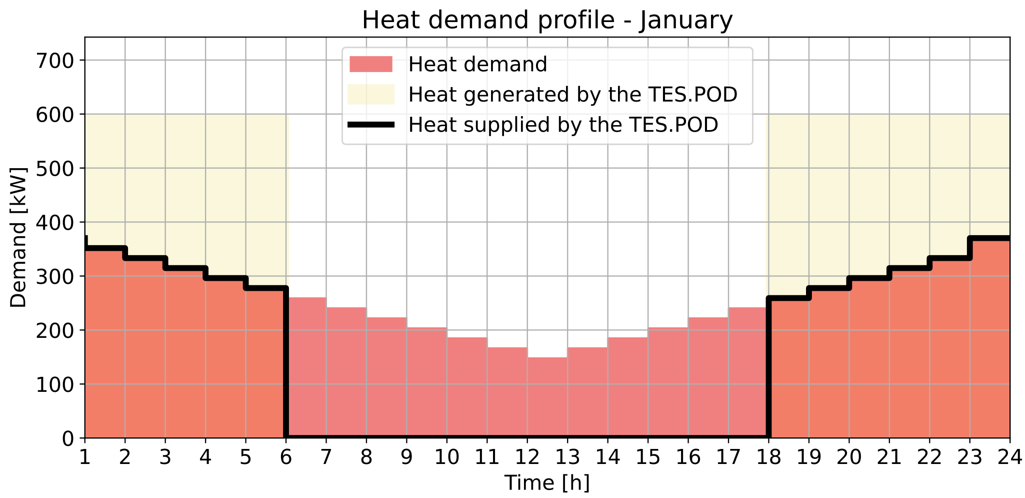

Figure 50: Heat demand profile for January with 100 % heat to electricity demand for the greenhouse case study.

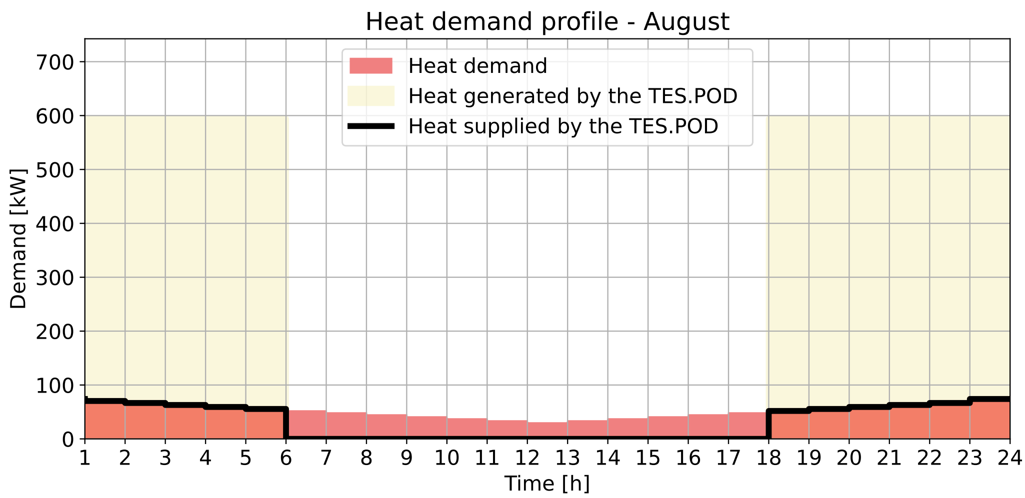

Figure 51: Heat demand profile for August with 100 % heat to electricity demand for the greenhouse case study.

The energy system is assumed to be supplied with heat from a natural gas boiler and electricity from the grid. Grid electricity and natural gas prices are assumed to be between 80 and 140 $\frac{USD}{MWh}$ and 13.6 to 54.6 $\frac{USD}{MWh}$, respectively. Boiler efficiency is assumed to be 90 %. The following results are modelled with an assumed constant

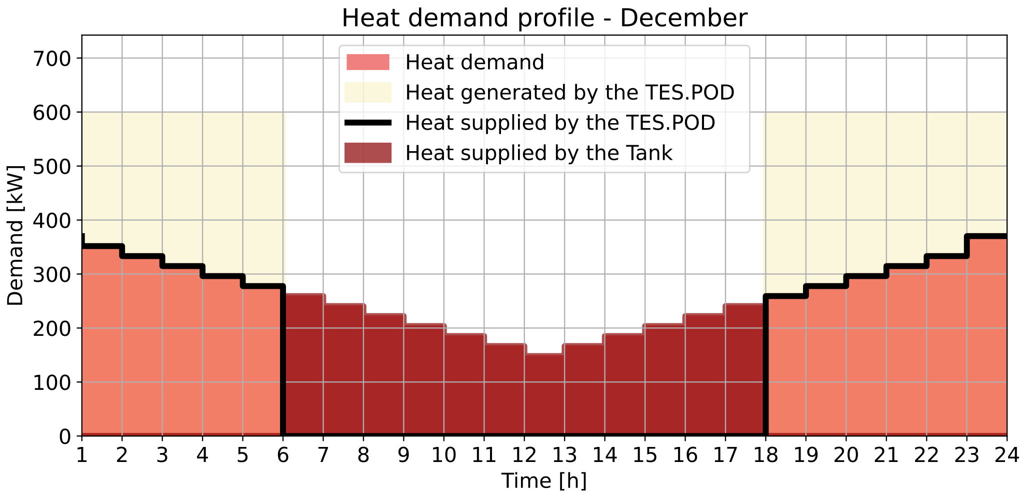

Figure 52: Heat demand profile for December with 100 % heat to electricity demand, including a hot water storage tank for the greenhouse case study.

daily electricity demand profile in figure 47, using calculated average values.

8.1.2. Results

The model was applied to the application with the TES.POD and solar power integration. The cost of electricity from the grid and natural gas were assumed fixed at 110 $\frac{USD}{MWh}$ and 40 $\frac{USD}{MWh}$, respectively. The heat to electricity demand percentage is set at 100 % and the electricity demand profile is assumed constant with calculated average values of the provided data depicted in figure 46. Capital- and variable cost of the TES.POD were assumed at 100 % of their default values. The same applies to the solar PV's at 850 $\frac{USD}{kW}$ and 10 $\frac{USD}{kWyr}$, respectively. The results are shown in figure 53 as a NPV timetable of 30 years, representing the lifetime of the TES.POD.

The total amount of electricity saved by supplying power at night is 1166 $\frac{MWh}{yr}$. Directly supplied heat from the TES.POD corresponds to 823 $\frac{MWh}{yr}$ and heat supplied by the hot water storage tank corresponds to 543 $\frac{MWh}{yr}$. The hot water storage tank's peak capacity is 1358 liters per day, which is the peak amount of water that must be stored during the months of January and December, when heat demand is at its maximum.

The fuel cost savings from supplying electricity and heat correspond to 128,159 $\frac{USD}{yr}$ and 60,724 $\frac{USD}{yr}$, respectively. These values are minimized by the OPEX values of solar PV's and the TES.POD to 76,740 $\frac{USD}{yr}$. The profits do not generate enough to overcome the investment, indicated by the negative NPV in the figure. As in the MED desalination case, natural gas is proven to be too cheap to generate enough monetary value by replacing it. The same can be concluded for the electricity coming from the grid. The assumption of lower to no heat demand during the summer months negatively affects the profitability of the heat generated from the TES.POD because most of the heat generated throughout the year is curtailed and of no value.

The change in NPV from calculating the HEX CAPEX using Azelio's estimate of 1000 $\frac{USD}{TES.POD}$ instead of using the equation found in the literature has a negligible effect, resulting in a one percent increase.

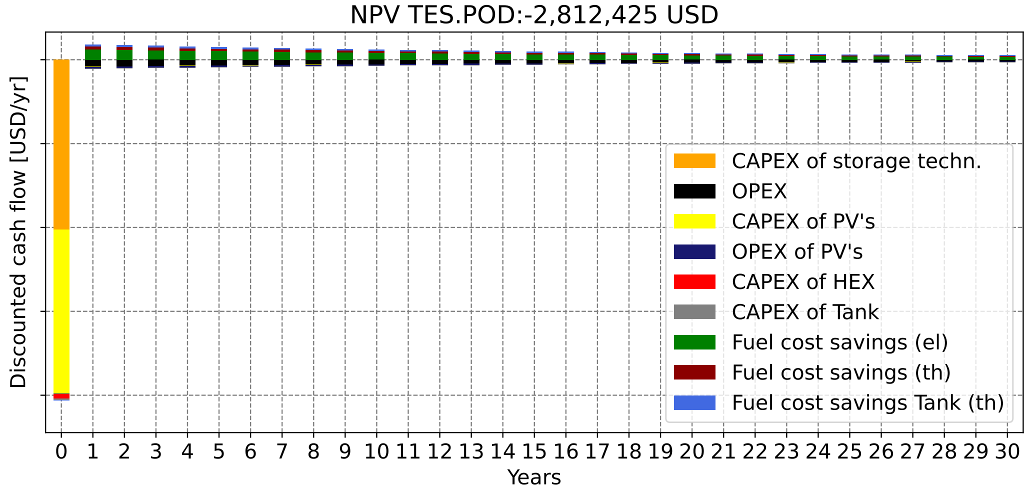

Figure 53: Cash flow diagram for the TES.POD in the Greenhouse case study with 100 % heat to electricity demand at a grid electricity price and natural gas price of 110 & 40 USD/MWh, respectively.

8.1.3. Sensitivity Analysis

Through a sensitivity analysis, a number of factors were investigated. Figure 54 shows the results of the NPV calculations for various heat to electricity demand percentages between 100, 50, and 20 %. Economics of the TES.POD as well as solar PV's are set at default.

The NPV's are plotted across a range of natural gas prices from 10 to 60 $\frac{USD}{MWh}$. The previous investigated scenarios generated heat and electricity with one fuel source, either natural gas or diesel. In this application, the source of electricity and heat generation of the existing system differ from each other. Hence, the effect of varying grid electricity prices cannot be plotted on the same x axis. The influence of changing grid electricity prices is depicted in color-coded lines.

The lines in red represent the results for a fixed grid electricity price of 80 $\frac{USD}{MWh}$ and the lines in green for a price of 120 $\frac{USD}{MWh}$. Within both colours, the shade of the colour depicts the change in heat to electricity demand percentages. As the lines become lighter, the heat-to-electricity demand percentage rises from 20 % to 100 %.

As expected, higher heat to electricity demand percentages result in higher heat

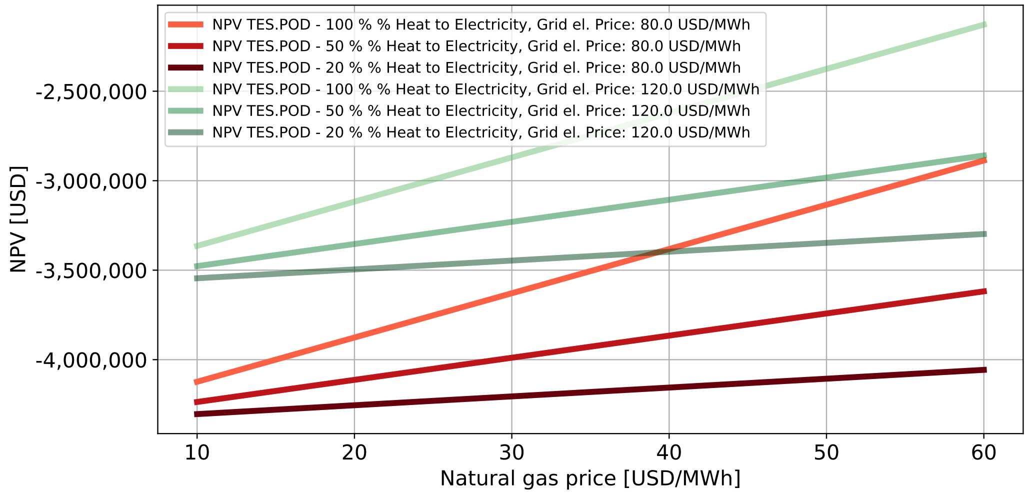

Figure 54: NPV results of the TES.POD in the Greenhouse case study for various heat to electricity scenarios for two different grid electricity prices, over a range of fuel prices. A hot water storage tank is included.

demands, which improves the TES.POD profitability. The same applies to higher electricity grid and natural gas prices. However, the results across all scenarios are negative, which indicates, as mentioned in section 8.1.2, that the fuel cost savings/ grid electricity savings are not enough to create enough monetary value to justify the investment from a purely economic point of view.

Figures 55 and 56 show the results of investigating varying the economic parameters capital- and variable cost of the TES.POD from default value of 100 % down to 60 %, respectively. The remaining parameters are unchanged. The heat to electricity demand percentage is set to 100 %. Again, the influence of changing grid electricity prices is depicted in color-coded lines. Darker shaded lines illustrate the results of lowering capital- and variable cost, respectively.

Both figures show that the profitability of the investment is unchanged. As expected, with declining cost percentages from 100 to 60 percent, the NPV's increase in value but remain negative.

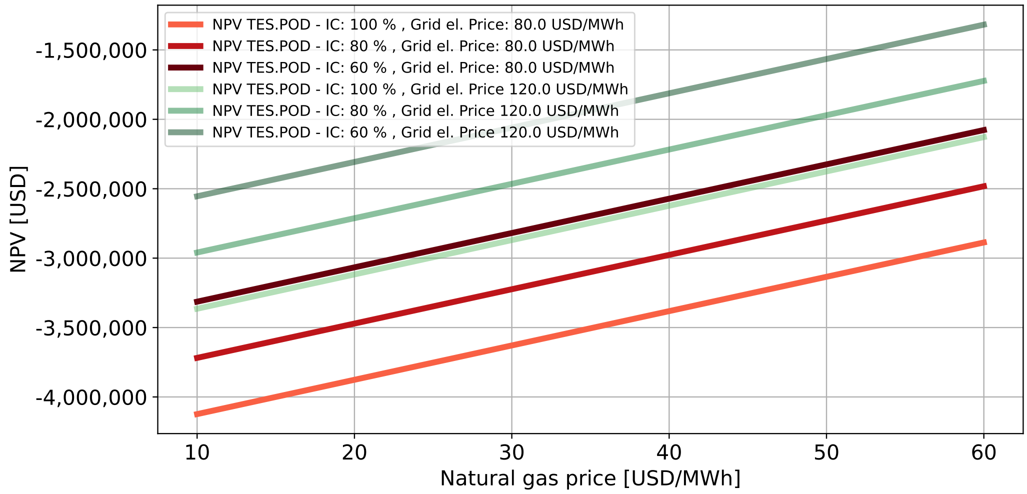

Figure 55: NPV results of the TES.POD in the Greenhouse case study for various capital costs IC scenarios for two different grid electricity prices, over a range of fuel prices. A hot water storage tank is included.

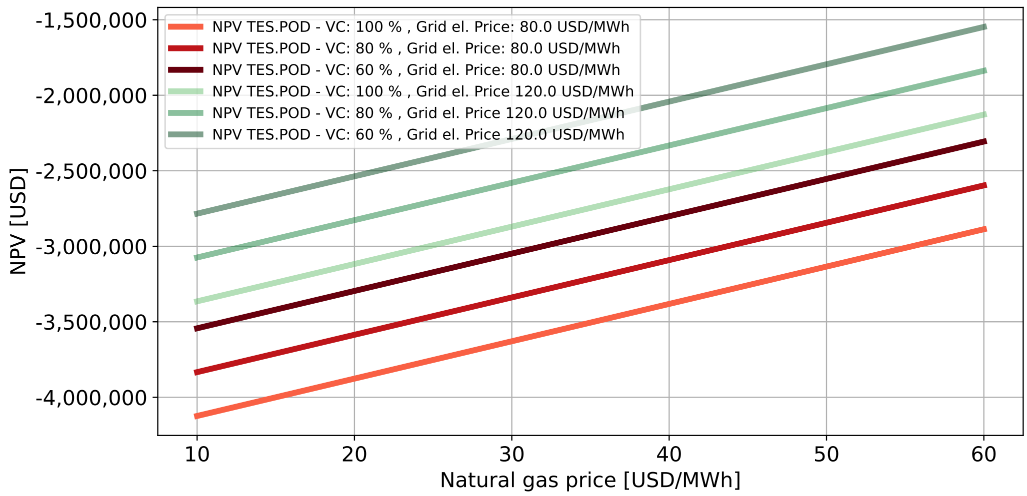

Figure 56: NPV results of the TES.POD in the Greenhouse case study for various variable costs VC scenarios for two different grid electricity prices, over a range of fuel prices. A hot water storage tank is included.

8.1.4. Final remarks

From an economic perspective, it can be concluded that the TES.POD investment turns out not to be justified for the specific greenhouse customer, assuming the heat demand profiles reflect the real demand of the customer reasonably and considering that other economic factors, such as repurchasing the boiler due to its shorter lifetime than the TES.POD, are neglected.

The assumed low to non-existent heat demand in the summer months limits the usage of the heat from the TES.POD. Although heat and electricity are demanded, the alternative options to provide both are too cost-efficient to justify the investment.

However, the customer's incentives to purchase the TES.POD are sustainability and grid uncertainties. Both of these factors are reasonable motivations, but they are subjective and difficult to quantify monetarily.

Conclusion

This thesis was done in cooperation with Azelio AB with the aim of identifying future business opportunities by investigating the economic value of integrating Azelio's TES.Pod, which operates in CHP mode, into an application's energy system.

This was done by constructing a mathematical model in Python that allowed for the techno-economic analysis of an energy storage system by applying fundamental thermodynamic and economic calculations. Potential applications were investigated by assuming solar power input and the energy storage system will be introduced as a green retrofit, replacing the existing energy system as much as possible by providing electricity and heat. The avoided cost of supplying and replacing energy is used as the basis to evaluate the investment in the storage system.

It was developed to function as a tool, delivering preliminary results of potential applications before more detailed but computationally more intensive modelling processes are applied. The model is limited by assuming fixed operational hours, a constant solar power output, and evaluating the investment only via a Net Present Value calculation. The model's applicability is restricted since it assumes a green retrofit of the application's energy system and does not create an energy system from scratch. Hence, it does not include other economic parameters than fuel cost and efficiency, such as the capital cost of alternative energy-generating technologies.

Furthermore, other economic incentives, such as CO_2 avoidance costs and tax benefits, are not included due to uncertainties, lack of data, and regional dependence. Lastly, the Net Present Value alone cannot determine if an investment is made or not because intangible purchase incentives which are hardly quantifiable, such as sustainability of materials compared to other energy storage solutions, are not represented in the model. A resulting negative NPV indicates unprofitability but excludes other potential reasons for purchase. It is suggested to use the model for comparison purposes between various competing energy storage technologies so that some of the intangible incentives can be accounted for and a better understanding of market standing can be acquired.

Throughout the thesis, the most time consuming process was finding the required data to apply the model for the investigated application. With the resources available, discovering process schematics, heat and electricity demand profiles, describing the energy system enough to create justifiable assumptions to develop a case where the model can be applied to, was time consuming and more than often failed.

The model was successfully applied in three different applications within distinct industry sectors. Hence, future work suggestions include, conducting more detailed modelling while obtaining more data, clarifying some of the assumptions made due to a lack of data.

List of Figures

List of Tables

References

Water Desalination Market Report. Visiongain Research Inc. URL https://www.visiongain.com/.

Techno-economic assessment and environmental impacts of desalination technologies. *Desalination*, 266(1):263–273, 2011. ISSN 0011-9164. doi: https://doi.org/10.1016/j.desal.2010.08.035. URL https://www.sciencedirect.com/science/article/pii/S0011916410006296.

Thermal Energy Storage Market Research Report by Material, by Technology, by Application, by End User, by Region - Global Forecast to 2027 - Cumulative Impact of COVID-19, 2021. URL https://www.globenewswire.com/news-release/2021/01/13/2157662/0/en/Thermal-Energy-Storage-Market-Research-Report-by-Material-by-Technology-by-Application-by-End-User-Global-Forecast-to-2025-Cumulative-Impact-of-COVID-19.html.

Energy storage on demand: Thermal energy storage development, materials, design, and integration challenges. *Energy Storage Materials*, 46:192–222, 2022. ISSN 2405-8297. doi: https://doi.org/10.1016/j.ensm.2022.01.017. URL https://www.sciencedirect.com/science/article/pii/S2405829722000174.

ABC News. Is desalination the answer to California's drought? Here's what experts say, 2021. URL https://abc7news.com/california-drought-water-shortages-seawater-desalination-brackish/10900176/.

A. Al-Karaghouli and L. L. Kazmerski. Energy consumption and water production cost of conventional and renewable-energy-powered desalination processes. *Renewable and Sustainable Energy Reviews*, 24:343–356, 2013. ISSN 1364-0321. doi: https://doi.org/10.1016/j.rser.2012.12.064. URL https://www.sciencedirect.com/science/article/pii/S1364032113000208.

B. Anand, R. Shankar, S. Murugavelh, W. Rivera, K. M. Prasad, and R. Nagarajan. A review on solar photovoltaic thermal integrated desalination technologies. *Renewable and Sustainable Energy Reviews*, 141:110787, 2021.

M. Ashourian, S. Cherati, A. Mohd Zin, N. Niknam, A. Mokhtar, and M. Anwari. Optimal green energy management for island resorts in malaysia. *Renewable Energy*, 51:36–45, 2013. ISSN 0960-1481. doi: https://doi.org/10.1016/j.renene.2012.08.056. URL `https://www.sciencedirect.com/science/article/pii/S0960148112005265`.

N. I. H. A. Aziz and M. M. Hanafiah. Application of life cycle assessment for desalination: Progress, challenges and future directions. *Environmental Pollution*, 268:115948, 2021.

T. Bartzanas, M. Tchamitchian, and C. Kittas. Influence of the heating method on greenhouse microclimate and energy consumption. *Biosystems Engineering*, 91(4):487–499, 2005. ISSN 1537-5110. doi: https://doi.org/10.1016/j.biosystemseng.2005.04.012. URL `https://www.sciencedirect.com/science/article/pii/S1537511005000784`.

D. Bauknecht and G. Brunekreeft. *Chapter 13 - Distributed Generation and the Regulation of Electricity Networks*. Elsevier Global Energy Policy and Economics Series. Elsevier, Oxford, 2008. doi: https://doi.org/10.1016/B978-008047172-3.50017-9. URL `https://www.sciencedirect.com/science/article/pii/B9780080471723500179`.

Bradley Corporation. US Groundwater temperatures. URL `https://www.bradleycorp.com/sizing-tankless-water-heaters/united-states-groundwater-temperatures`.

S. Bragg-Sitton. 13 - hybrid energy systems (hess) using small modular reactors (smrs). In M. D. Carelli and D. T. Ingersoll, editors, *Handbook of Small Modular Nuclear Reactors*, Woodhead Publishing Series in Energy, pages 319–350. Woodhead Publishing, 2015. ISBN 978-0-85709-851-1. doi: https://doi.org/10.1533/9780857098535.3.319. URL `https://www.sciencedirect.com/science/article/pii/B9780857098511500133`.

P. Breeze. Chapter 8 - hydrogen energy storage. In P. Breeze, editor, *Power System Energy Storage Technologies*, pages 69–77. Academic Press, 2018. ISBN 978-0-12-812902-9. doi: https://doi.org/10.1016/B978-0-12-

812902-9.00008-0. URL https://www.sciencedirect.com/science/article/pii/B9780128129029000080.

X. Cao, X. Huang, P. Liang, K. Xiao, Y. Zhou, X. Zhang, and B. E. Logan. A new method for water desalination using microbial desalination cells. *Environmental science & technology*, 43(18):7148–7152, 2009.

B. Cardoso, A. Gaspar, J. Góis, and E. Rodrigues. Energy and water consumption characterization of portuguese indoor swimming pools. 06 2018. doi: 10.31224/osf.io/e8awk.

C. E. Clark and J. A. Veil. Produced water volumes and management practices in the united states., 2009.

CTCN, UN Climate Technology Centre & Network. Compressed Air Energy Storage (CAES). URL https://www.ctc-n.org/technologies/compressed-air-energy-storage-caes.

Current Results. Phoenix, Arizona monthly temperature profile data. URL https://www.currentresults.com/Weather/Arizona/Places/phoenix-temperatures-by-month-average.php.

H. R. Dastgerdi, P. B. Whittaker, and H. T. Chua. New med based desalination process for low grade waste heat. *Desalination*, 395:57–71, 2016. ISSN 0011-9164. doi: https://doi.org/10.1016/j.desal.2016.05.022. URL https://www.sciencedirect.com/science/article/pii/S0011916416304350.

G.-C. J. R. Delgado Marín, José Pablo. Dynamic simulation model and empirical validation for estimating thermal energy demand in indoor swimming pools. 2020.

O. Dumont, G. F. Frate, A. Pillai, S. Lecompte, M. De paepe, and V. Lemort. *Carnot battery technology: A state-of-the-art review*, volume 32. 2020. doi: https://doi.org/10.1016/j.est.2020.101756. URL https://www.sciencedirect.com/science/article/pii/S2352152X20315930.

H. T. El-Dessouky and H. M. Ettouney. *Fundamentals of salt water desalination.* Elsevier, 2002.

K. Elsaid, E. Taha Sayed, B. A. Yousef, M. Kamal Hussien Rabaia, M. Ali Abdelkareem, and A. Olabi. Recent progress on the utilization of waste heat for desalination: A review. *Energy Conversion and Management*, 221:113105, 2020. ISSN 0196-8904. doi: https://doi.org/10.1016/j.enconman.2020.113105. URL `https://www.sciencedirect.com/science/article/pii/S019689042030649X`.

Engevity. Australian Energy Market Review December 2021 Context and Opportunities for Azelio's TES.POD, 2021. URL `https://www.engevity.com.au/`.

ENTSOE. URL `https://transparency.entsoe.eu/dashboard/show`.

EPA, United States Environmental Protection Agency. Electricity Storage. URL `https://www.epa.gov/energy/electricity-storage`.

H. Gadd and S. Werner. Achieving low return temperatures from district heating substations. *Applied Energy*, 136:59–67, 2014. ISSN 0306-2619. doi: https://doi.org/10.1016/j.apenergy.2014.09.022. URL `https://www.sciencedirect.com/science/article/pii/S0306261914009696`.

A. Goldstein. Federal policy to accelerate innovation in long-duration energy storage: The case for flow batteries. 2021.

M. A. Gonzalez-Salazar, T. Kirsten, and L. Prchlik. Review of the operational flexibility and emissions of gas- and coal-fired power plants in a future with growing renewables. *Renewable and Sustainable Energy Reviews*, 82:1497–1513, 2018. ISSN 1364-0321. doi: https://doi.org/10.1016/j.rser.2017.05.278. URL `https://www.sciencedirect.com/science/article/pii/S1364032117309206`.

L. Göransson. Variability and variation management in a renewable electricity system -large-scale wind- and solar power deployment in europe.

S. Hall, S. Ahmad, and R. Smith. Capital cost targets for heat exchanger networks comprising mixed materials of construction, pressure ratings and exchanger types. *Computers Chemical Engineering*, 14(3):319–335, 1990. ISSN 0098-1354. doi: https://doi.org/10.1016/0098-1354(90)87069-2. URL `https://www.sciencedirect.com/science/article/pii/0098135490870692`.

Heritage Water Tanks. The Ultimate Guide To Water Tank Prices. URL https://heritagetanks.com.au/water-tank-prices/.

F. Hesari, F. Salimnezhad, M. H. Khoshgoftar Manesh, and M. Morad. A novel configuration for low-grade heat-driven desalination based on cascade med. *Energy*, 229, 04 2021. doi: 10.1016/j.energy.2021.120657.

IEA. World Energy Outlook 2021, IEA, a. URL https://www.iea.org/reports/world-energy-outlook-2021.

IEA. Energy Storage, b. URL https://www.iea.org/reports/district-heating.

IEA. Global Energy Review 2020, c. URL https://www.iea.org/reports/global-energy-review-2020.

IEA. District Heating, d. URL https://www.iea.org/reports/energy-storage.

IRENA, International Renewable Energy Agency. Heating & Cooling, a. URL https://www.irena.org/heatingcooling.

IRENA, International Renewable Energy Agency. Renewable Energy Opportunities for Island Tourism, b. URL https://www.irena.org/publications/2014/Aug/Renewable-Energy-Opportunities-for-Island-Tourism.

F. J. Jamshidian, S. Gorjian, and M. Shafieefar. Techno-economic assessment of a hybrid ro-med desalination plant integrated with a solar chp system. *Energy Conversion and Management*, 251:114985, 2022. ISSN 0196-8904. doi: https://doi.org/10.1016/j.enconman.2021.114985. URL https://www.sciencedirect.com/science/article/pii/S0196890421011614.

P. S. Kauranen, P. D. Lund, J. R. Leppänen, and D. J. Spiers. Hydrogen energy storage for photovoltaic power systems. In A. Luque, G. Sala, W. Palz, G. Dos Santos, and P. Helm, editors, *Tenth E.C. Photovoltaic Solar Energy Conference*, pages 476–479, Dordrecht, 1991. Springer Netherlands.

J. Kim, K. Park, and S. Hong. Application of two-stage reverse osmosis system for desalination of high-salinity and high-temperature seawater with improved stability and performance. *Desalination*, 492:114645, 2020. ISSN 0011-9164. doi: https://doi.org/10.1016/j.desal.2020.114645. URL `https://www.sciencedirect.com/science/article/pii/S0011916420313230`.

M. Lantz. Azelio's thermal battery for combined heat and power – a thermo-economic and market research study. 2020.

LDES Council. FLAGSHIP 2021 NET-ZERO POWER REPORT, 2022. URL `https://www.ldescouncil.com/`.

S. Lin, H. Zhao, L. Zhu, T. He, S. Chen, C. Gao, and L. Zhang. Seawater desalination technology and engineering in china: A review. *Desalination*, 498:114728, 2021. ISSN 0011-9164. doi: https://doi.org/10.1016/j.desal.2020.114728. URL `https://www.sciencedirect.com/science/article/pii/S0011916420314065`.

N. McIlwaine, A. M. Foley, D. J. Morrow, D. Al Kez, C. Zhang, X. Lu, and R. J. Best. A state-of-the-art techno-economic review of distributed and embedded energy storage for energy systems. *Energy*, 229:120461, 2021. ISSN 0360-5442. doi: https://doi.org/10.1016/j.energy.2021.120461. URL `https://www.sciencedirect.com/science/article/pii/S0360544221007106`.

J. McTigue. Crescent dunes solar energy facility, usa "carnot batteries" for electricity storage. 2019.

K. Mongird, V. Viswanathan, J. Alam, C. Vartanian, V. Sprenkle, and R. Baxter. 2020 grid energy storage technology cost and performance assessment. *Energy*, 2020, 2020.

R. Nielsen and S. Thorsteinsson. Lecture notes in Photovoltaics System course. URL `https://www.coursera.org/`.

NREL. Cost Projections for Utility-Scale Battery Storage: 2021 Update, a. URL `https://www.nrel.gov/docs/fy21osti/79236.pdf`.

NREL. Utility-Scale Battery Storage, b. URL https://atb.nrel.gov/electricity/2021/utility-scale_battery_storage.

Oil Crude Price. Natural Gas Price today. URL https://www.oilcrudeprice.com/natural-gas-price/.

H. Ozturk and K. Kucukerdem. Determination of heating requirements and energy consumption of greenhouses in adana region of turkey. *AgroLife Scientific Journal*, 5:157–160, 06 2016.

G. Palmer and J. Floyd. *The Role of Storage in Management of Electricity Grids*, pages 89–108. Springer International Publishing, Cham, 2020. ISBN 978-3-030-33093-4. doi: 10.1007/978-3-030-33093-4_6. URL https://doi.org/10.1007/978-3-030-33093-4_6.

K. Rahman, S. Rahman, K. Ullah, Y. S. Hajimolana, W. Hew, and M. Hussain. Economic feasibility analysis of a solar energy and solid oxide fuel cell-based cogeneration system in malaysia. *Clean Technologies and Environmental Policy*, 18, 03 2016. doi: 10.1007/s10098-015-1050-6.

V. Rudolf and K. D. Papastergiou. Financial analysis of utility scale photovoltaic plants with battery energy storage. *Energy Policy*, 63:139–146, 2013. ISSN 0301-4215. doi: https://doi.org/10.1016/j.enpol.2013.08.025. URL https://www.sciencedirect.com/science/article/pii/S0301421513008185.

SEIA, Solar Energy Industries Association. Solar Investment Tax Credit. URL https://www.seia.org/initiatives/solar-investment-tax-credit-itc.

S. Shalaby, S. W. Sharshir, A. Kabeel, A. Kandeal, H. Abosheiasha, M. Abdelgaied, M. H. Hamed, and N. Yang. Reverse osmosis desalination systems powered by solar energy: Preheating techniques and brine disposal challenges–a detailed review. *Energy Conversion and Management*, 251:114971, 2022.

P. Sinha and K. K. Kar. *Introduction to Supercapacitors*, pages 1–28. Springer International Publishing, Cham, 2020.

V. Smil. *Energy transitions: global and national perspectives*. ABC-CLIO, 2016.

K. A. Sören Amelang. The causes and effects of negative power prices. Clean Energy Wire, Journalism of energy transition. URL `https://www.cleanenergywire.org/factsheets/why-power-prices-turn-negativ`.

H. Tahir, M. S. Khan, M. M. Ullah, M. Ali, and M. Shakaib. Influence of operating temperature range on the performance of multi-effect desalination (med) plant. *Materials Today: Proceedings*, 2021. ISSN 2214-7853. doi: https://doi.org/10.1016/j.matpr.2021.11.455. URL `https://www.sciencedirect.com/science/article/pii/S2214785321074782`.

TEMPO. Network Optimisation – Digitalisation. URL `https://www.tempo-dhc.eu/network-optimisation-digitalisation/`.

R. Turconi, A. Boldrin, and T. Astrup. Life cycle assessment (lca) of electricity generation technologies: Overview, comparability and limitations. *Renewable and Sustainable Energy Reviews*, 28:555–565, 2013. ISSN 1364-0321. doi: https://doi.org/10.1016/j.rser.2013.08.013. URL `https://www.sciencedirect.com/science/article/pii/S1364032113005534`.

U.S. Energy Information Administration. URL `https://www.eia.gov/`.

P. Van Beveren, J. Bontsema, G. Van Straten, and E. Van Henten. Minimal heating and cooling in a modern rose greenhouse. *Applied Energy*, 137:97–109, 2015. ISSN 0306-2619. doi: https://doi.org/10.1016/j.apenergy.2014.09.083. URL `https://www.sciencedirect.com/science/article/pii/S0306261914010319`.

P. van Beveren, J. Bontsema, G. van Straten, and E. van Henten. Optimal utilization of a boiler, combined heat and power installation, and heat buffers in horticultural greenhouses. *Computers and Electronics in Agriculture*, 162:1035–1048, 2019. ISSN 0168-1699. doi: https://doi.org/10.1016/j.compag.2019.05.040. URL `https://www.sciencedirect.com/science/article/pii/S0168169919302339`.

M. Varisco. A commercial thermal energy storage technology for chp and heat-only applications in industries: market research analysis and techno-economic assessment. 2021.

B. Weber, E. Cerro, I. G. Martínez, E. Rincón, and M. D. Duran. Efficient heat generation for resorts. *Energy Procedia*, 57:2666–2675, 2014. ISSN 1876-6102. doi: https://doi.org/10.1016/j.egypro.2014.10.278. URL `https://www.sciencedirect.com/science/article/pii/S1876610214016452`. 2013 ISES Solar World Congress.